TRACE CODE VALIDATION OF BOILING WATER REACTOR SPRAY COOLING INJECTION INTO A SVEA FUEL ASSEMBLY

BY

TRAVIS C. MUI

THESIS

Submitted in partial fulfillment of the requirements
for the degree of Master of Science in Nuclear, Plasma, and Radiological Engineering
in the Graduate College of the
University of Illinois at Urbana-Champaign, 2015

Urbana, Illinois

Master's Committee:

Assistant Professor Tomasz Kozlowski, Adviser
Assistant Professor Caleb Brooks

ABSTRACT

Best-estimate codes have been developed in the nuclear industry to design and license nuclear power plants to a greater degree of accuracy and safety assurance. Such codes necessitate efforts to qualify their validity, particularly with modeling the complex thermal-hydraulics phenomena associated with Loss-of-Coolant Accident (LOCA) scenarios. Emergency spray cooling injection is a safety feature implemented in many Boiling Water Reactor (BWR) designs to re-flood a reactor during an accident. Significant experimental work has qualified the efficacy of spray cooling, and ongoing computational modeling efforts strive to more accurately portray the phenomena involved. This thesis examines the physical phenomena pertaining to emergency spray cooling injection over SVEA-type fuel assemblies. The US NRC thermal-hydraulics code TRACE version 5.0 Patch 4 has been chosen to simulate the separate-effect tests performed by ASEA-ATOM. The computational model was evaluated by performing forward uncertainty quantification using Dakota as the analysis tool and code driver. 31 parameters were identified in the TRACE model input, 24 of which pertain to the developed input model and 7 of which pertain to the physical constitutive models used in TRACE. The developed model was able to provide a reasonable prediction of the trend of the transient peak cladding temperature. The most influential parameters from the uncertainty quantification model were the countercurrent flow limiting (CCFL) model constant and rod/wall emissivity, emphasizing that detailed understanding of CCFL and an accurately determined radiation model is essential for accurate simulation of emergency BWR spray cooling systems. For the physical model sensitivity coefficients, the TRACE model was particularly sensitive to the dispersed film flow boiling (DFFB) wall-liquid and single-phase wall-vapor heat transfer coefficients which correspond to the flow regime expected at the occurrence of peak cladding temperature in a BWR LOCA reflood scenario with spray cooling present.

ACKNOWLEDGEMENTS

I would like to express my earnest gratitude towards my advisor Professor Tomasz Kozlowski for his constant support, inspiration, and patience throughout the realization of this work. I thank him for his adept guidance into the field of computational safety analysis and the academic world. I would also like to thank Professor Caleb Brooks and Professor James Stubbins for their assessment and regarded perspectives in the review of this work.

I would also like to thank my colleagues Guojun Hu, George McKenzie, Xu Wu, Dr. Rabie Abu Saleem, and Daniel O'Grady for their thoughts and their company throughout the research and writing of this work. I would like to recognize all the faculty and staff of the Nuclear, Plasma, and Radiological Engineering department who have continuously aided and guided me since the very beginning of my freshman year. I would also like to thank Emma Palm and Peter Hedberg with the Swedish Radiation Safety Authority (Strålsäkerhetsmyndigheten) who provided the documentation from the SVEA spray cooling experiments and supported the basis for this work.

I thank my brothers, sisters, officers and pastors at Covenant Fellowship Church who have ceaselessly encouraged, prayed, and challenged me throughout my time in Champaign. I have whole-hearted thankfulness for my parents and my brother Byron, who have always encouraged me and without whom this work would not have been possible. Above all, I thank God, for by His grace this work was accomplished and to Him be all the glory.

CONTENTS

FIGURES

TABLES

1. INTRODUCTION

Safe and efficient operation of nuclear reactors relies significantly on an accurate understanding of the physical phenomena that occur during both normal and abnormal scenarios. To approve a nuclear reactor for operation, its design must demonstrate proper requirements to address all of these physical conditions, particularly during accident scenarios where complex interactions between several fundamental physical processes occur. Computational simulation of a nuclear reactor and its components provides an adept method for modeling and demonstrating these physical phenomena while mitigating the considerable costs of representative physical experimentation. A wide variety of simulation codes have been developed to assess accident scenarios and reactor performance, particularly in loss-of-coolant accident (LOCA) scenarios. The ability to capture the physical phenomena of LOCA conditions in a simulation has evolved as computational methods have become more effective and efficient alongside improved understanding of the physical processes. Verification and validation of these computational tools against comprehensive, detailed investigation of physical experimentation is necessary to provide an assurance in the capabilities of computational as the industry shifts from prior conservative evaluation models to increasingly accurate best-estimate models.

In a typical Boiling Water Reactor (BWR) design, several engineered safety features are implemented to respond to different accident conditions, with the primary goal of maintaining the reactor core in a cooled, contained state. BWR emergency core cooling system (ECCS) designs commonly incorporate a Low-Pressure Core Spray (LPCS) system that introduces coolant through spray nozzles directed to the top of the core, and are located in the upper plenum region. This design is effective for LOCA response, particularly during the initial refill and reflood stages of accident response where the goal

is limiting the peak cladding temperature rise in the core fuel rods. These types of spray cooling systems are found in most BWRs currently in operation, particularly those licensed in Sweden. At the time of their institution, spray cooling systems were qualified for operation through numerous integral and separate-effect test experiments, which were subsequently modeled with conservative evaluation models. The primary goal of these evaluation models was to provide an assessment tool to qualify reactor designs with a considerable margin to assure its safety and avoid under-prediction of safety-relevant parameters. This type of approach generally over-predicts safety parameters (such as cladding temperature) by assuming extreme model input conditions so that the worst-case scenario is consistently represented as a means of conservatively assessing safety margins [1].

However, with significant improvement of computational tools, the U.S. Nuclear Regulatory Commission (NRC) has endorsed a Best Estimate Plus Uncertainty (BEPU) approach for this type of modeling work over conservative evaluation methods [1]. The goal of BEPU methodologies aims to capture the physical phenomena as realistically as possible by implementing a wide range of modeling options and increasingly precise calculation methods to deal with a greater fidelity of physical phenomena. The present work specifically investigates the abilities of a thermal-hydraulics code designed with this approach. This work utilizes the US NRC-supported thermal-hydraulics code TRAC/RELAP Advanced Computational Engine (TRACE) to model the SVEA spray cooling experiment performed in 1986 by Asea-Atom [2] used to qualify spray cooling designs for Swedish BWR operating with SVEA-64 type fuel assemblies. However, the implementation of such detailed codes with numerous model options necessitates a study of the effects of modeling choices made by both user and code to determine their overall effect on the prediction performance of the computational model. The determination and reduction of such uncertainties has been an ongoing focus of the community involved with

development of these computational tools. The U.S. Department of Energy (DOE) Nuclear Energy Advanced Modeling and Simulation (NEAMS) program has greatly advocated this effort, with one such goal of implementing any incremental improvement of the knowledge-base of TH code parameters. In addition to the modeling work performed here with TRACE, uncertainty quantification is also performed on the TRACE computational model using Dakota as the uncertainty quantification tool and code driver. An effort is made to identify any sensitive parameters in the modeling of the experiment as well as in the physical empirical models that are used by TRACE to numerically evaluate two-phase flow by propagating these uncertain input parameters through the developed model.

1.1 Literature Review

A large-break LOCA in a BWR is a design-basis accident in which a double-ended guillotine break occurs in the largest pipe diameter, which is the inlet-end of the recirculation loop that is notably located at an elevation below the core but above the lower plenum. The LBLOCA scenario is generally broken down into three phases: blowdown, refill, and reflood. After the initiation of the accident and reactor scram, the reactor vessel undergoes depressurization (due to the break and an Automatic Depressurization System) and coolant inventory in the core is lost through the break during the blowdown phase [3]. The system is isolated by closing all valves, typically within 4 seconds of initiation. Due to depressurization, a large amount of fluid in the lower plenum flashes to steam that flows through the core and quenches the fuel during blowdown roughly 10 seconds into the transient. However, since this flow is limited, a boiling transition begins to occur as the core is again uncovered approximately 20 seconds in. The refill phase begins with actuation of the emergency core cooling system (ECCS), including core spray, within 35-40 seconds depending on the design of the system. As the core begins to refill, the core continues to heat up due to decay heat while there is still very little liquid inventory. During this refill phase, heat transfer will be dominated by steam convection and radiation heat

transfer, largely determining the rate at which the cladding temperature will rise up and ultimately the peak cladding temperature. When ECCS mechanisms reach their rated flow capacities, the reflood phase begins and continues until the entire core is rewetted and liquid inventory is re-established in the core. During the refill-reflood phase, the performance of ECCS and core heat transfer is especially important as the core reaches its most extreme conditions during this period. Countercurrent flow limiting during this phase may result in falling spray coolant droplets being entrained in the upward steam flow [4], or spray coolant pooling in the upper plenum being prevented from entering the core region [5].

Several different mechanisms govern and affect the heat transfer capability of the core coolant during the different phases of a LOCA. Of primary interest here are the phenomena directly related to spray cooling, which include both the heat transfer characteristics of different fluid flow types, and other phenomena that affect the mixing of fluid flow in the core region. Transient heat transfer of spray droplets on rod bundles is a primary area of interest when evaluating the performance of spray cooling systems for nuclear reactors. Yamanouchi [6] developed a classical physical model to describe the transient phenomena of rod bundles under spray cooling. In practice, the Yamanouchi model itself is not a physical model used in computational simulations of spray cooling thermal-hydraulics conditions, but provides a basis for understanding the general trend of spray cooling wet front progression and for comparison to modeled effects.

From the Yamanouchi model, typical rod wall temperature transients under spray cooling (Figure 1) can be broken down into three stages:

Stage I: Dry rods heating up before initiation of spraying results in a dominantly linear increase in wall temperature with time. Heat transfer at this stage following blowdown core uncovery is by steam convection and radiation.

Stage II: After spraying initiates, heat transfer through mist cooling takes place until sufficient liquid begins to progress through the rod channel where film boiling will start to decrease the temperature.

Stage III: Rapid cooling and significant drops in wall temperature occur as the wet front of the spray water film migrates and covers the wall surface, leading to nucleate boiling and convection to liquid.

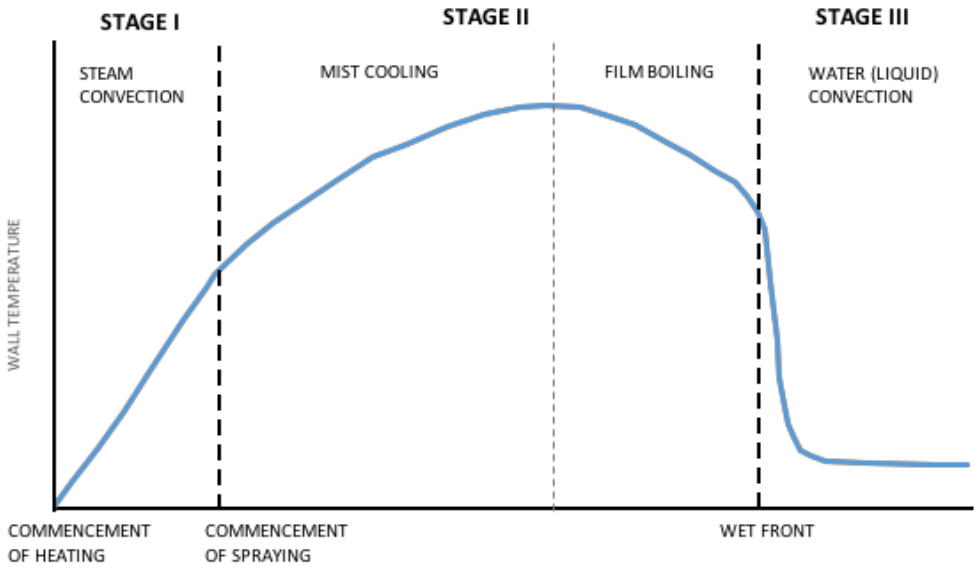

Figure 1. Rod wall temperature cooling progression by spray cooling over three stages of heat transfer. Initial stage of heating has linear temperature increase, with second stage reaching the peak temperature with some heat removal, and the third stage where water film is established with rapid cooling. [6]

This type of transient cooling behavior is widely observed in integral-test experiments designed to simulate a full BWR LOCA, including the SVEA-fuel spray cooling experiments performed by Asea-Atom [2]. By this model, peak cladding temperature (PCT) usually occurs in Stage II, where spray cooling has initiated and introduced some fluid flow into the fuel bundle region, but has not yet established a water film that leads to the significant convective cooling that occurs in Stage III. Phenomena that affect the rate

at which a water film can be established on the rod surface have significant impact on ECCS performance. The model set forth by Yamanouchi formed the basis for conservative evaluation modeling. Principal studies of BWR spray cooling efficacy quantified the model through the BWR Full-Length Emergency Core Heat Transfer (BWR-FLECHT) experiment performed by General Electric in 1968-1970 [7]. Using these experiments and models, the US NRC established guidelines for licensing of nuclear reactors and are documented in the 10 CFR 50 Appendix K [8]. These guidelines describe the heat transfer coefficients that are to be applied to BWR fuel assemblies under spray cooling during a LOCA scenario as a conservative means to assess the cladding temperature rise. From the initial BWR-FLECHT experiment, these heat transfer coefficients were determined from entire-assembly energy measurements and response calculations solely at the axial mid-plane.

Counter-Current Flow Limiting (CCFL) is a phenomenon that occurs during BWR LOCA and affects channel fluid flow properties. In this phenomenon, the spray water droplets and a rod-surface film flows in a downward direction (due to gravity) clinging to the rod surface while the channel region encounters steam vapor flow in an upward direction [9]. This steam flow can be attributed to boiling at lower fuel rod elevations in the core [10], or it could also be attributed to steam production from water in the lower plenum flashing as the reactor depressurizes [11]. If the upward vapor flow is sufficient, it can entrain the falling droplets and sometimes the downward liquid film flow, resulting in upward flow reversal (Figure 2). This effect is significant and considerable for a BWR under LOCA conditions, as it prevents emergency coolant from entering core regions experiencing this CCFL effect. During refill-reflood phase, CCFL was observed to occur at the upper tie plate region, where steam up-flow prevents the spray water from migrating into the fuel bundles.

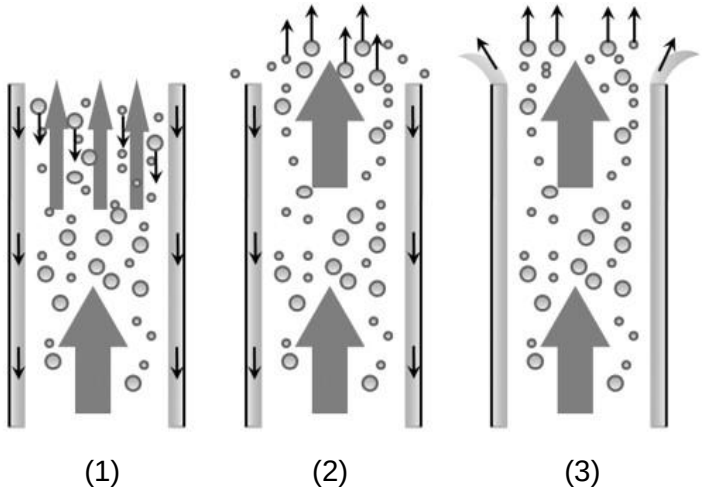

Figure 2. Progression of counter-current flow in a vertical channel with dispersed liquid phase, starting with (A) counter-current downward annular-mist flow progressing to (B) entrainment of droplets in the upward vapor steam flow and furthermore to (C) concurrent upward annular-mist flow [4].

In response to this phenomenon, General Electric and the Electric Power Research Institute investigated this ECCS mixing phenomena under the BWR Refill-Reflood Program at the Steam Sector Test Facility (SSTF) [5] which modeled a 30° sector of a GE BWR upper plenum region. The findings concluded that during the initial stages of spray water entering the upper plenum, CCFL from steam flow upward through the core and upper tie plate prevents water from entering the central region of the core, resulting in a spray water pool that collects in the upper plenum. As increased cooling occurs in the periphery of the core, the bulk fluid temperature of the upper plenum pooled coolant approaches saturation and CCFL breakdown occurs, allowing spray water to enter into the fuel bundles from the periphery. From this initial breakdown, the subsequent cooling then results in the CCFL effect breaking down and allowing water into the core, progressing from the periphery to the center of the upper tie plate [5]. This pooling of water in the upper plenum results in delayed progression to Stage III cooling of fuel rods in the central fuel bundles during the Refill phase, and prolonged Stage II cooling where PCT occurs (Figure 1). However, it is shown that the cooling that occurs from the concurrent

steam flow through the central bundles is comparable, if not greater than spray heat transfer [5]. With respect to the discontinuous liquid phase (i.e. droplets in steam flow), CCFL will tend to mitigate the downward progression of the spray flow in general in the bundle channel, which delays the delivery of emergency coolant to the middle and lower levels of the core where PCT tends to occur. As a result, the heat transfer mechanisms that dominate the central fuel bundles experiencing CCFL phenomena will be governed by convection to vapor flow in the channel and by radiation heat transfer. These phenomenological sensitivities thus occur during the initial period of reflood prior to the incipience of PCT, corresponding to the end of Stage I and the early portion of Stage II spray cooling.

The experiment and analysis of the SVEA spray cooling tests during the late 1980s was performed by Asea-Atom (under ABB Atom, now Westinghouse Electric Sweden AB). At the time of the data analysis and code validation, the code of choice was GOBLIN/DRAGON, a proprietary code developed by ABB Atom [3]. GOBLIN is a system 1-D thermal-hydraulics code that encompasses all the components of a reactor loop, with the entire core as a component. DRAGON is a subset of GOBLIN that performs detailed analysis for a chosen bundle (typically the hot channel in the reactor core) using the boundary conditions provided by GOBLIN [16]. To perform the evaluation model analysis of the SVEA spray cooling tests, DRAGON was used to simulate the SVEA test bundle at the mid-plane elevation [3]. Heat transfer coefficients derived from the findings of BWR-FLECHT and GÖTA experiments were applied in the model to calculate the peak cladding temperatures of the three rod positions (corner, side, and central). These conservative models in both cases were able to predict the peak cladding temperature with relatively good accuracy, and the time to quench (middle and end of Stage II spray cooling) for the standard case (Test 015) also gave comparable results [3].

The GOBLIN code was further developed later on by ABB Atom and evolved as a best-estimate code (GOBLIN-BE). Further validation studies were performed on a selection of SVEA spray cooling tests, and an uncertainty analysis was performed on the capability of predicting PCT [12]. GOBLIN-BE performs a more detailed analysis of the core with a fully implicit hydraulics model (which accounts for liquid film and droplet models, along with quench front tracking) and a thermal model that divides heat transfer into wall to liquid/vapor convection and wall to wall/liquid/vapor radiation models. This model is able to predict the transient axial temperature distribution (not just the midplane level), and was able to verify PCT and quench front propagation phenomena by directly comparing to the thermocouple measurements made at different bundle elevations. Overall, the comparisons demonstrated the model's capability of predicting PCT at various elevations and capturing of quench propagation. The areas of modeling difficulty were in under-predicting PCT at upper rod positions for low power tests and over-prediction of PCT at lower rod positions due to the CCFL effect that was predicted by the code but not observed in the test [12]. The modeling uncertainties were assessed for the total bundle power, bundle internal power distribution, axial power distribution, spray cooling flow rate, dry surface emissivity, and nodalization parameters. A sensitivity assessment for CCFL was not made. Overall, the rod emissivity contributed the highest uncertainty (5%), indicating the importance of the radiation model when performing a best-estimate analysis. From these parameters, the total GOBLIN-BE PCT uncertainty was cited with a bias of 16.3° C and standard deviation of 31.1° C at 95% single-sided confidence level.

An analysis was performed by Racca and Kozlowski [13] to verify TRACE modeling capabilities against the test results from the GÖTA spray cooling experiments, which were a series of tests also performed by Asea-Atom to qualify spray cooling for standard 8 x 8 BWR fuel assemblies licensed for Swedish BWRs. The effort compared two component combinations to model the test bundle. The first setup utilized two PIPE components to

model the rod bundle channel and the bypass channel. Two HTSTR heat structure components were used to model the inner and outer walls and six HTSTR components modeled six rod groups in the 8x8 rod bundle. The second setup utilized a PIPE component for the bypass channel and a CHAN (channel) component to model the heater rods. FILL and BREAK components simulate the spray coolant flow injection and drain boundary conditions, respectively. When evaluating the radiation model, it was found that the CHAN component Monte Carlo-based automatic radiation model's lack of capability in defining the canister wall and inner bypass channel surface resulted in over-prediction of the canister wall temperatures. Decreasing the emissivity of the canister wall to absorb less heat during simulation mitigated this lack of modeling detail. The PIPE component required user-defined parameters for the radiation model, and it was identified that TRACE is unable to define radiation models for rods within the same HTSTR (heat structure) group (the HTSTR cannot "see itself"), which limits a major radiation heat transfer component. TRACE was able to model the peak cladding temperature transients well in comparison to the GÖTA test results, but there were limitations in the accuracy of the model. TRACE was unable to capture the radial distribution of PCT across the fuel bundle that occurs with different flow regimes (primarily falling film on the periphery channels and upflowing steam in the central channels) since the PIPE and CHAN components use 1D approximation for the conservation equations. As such, the simulated temperatures were similar across the entire rod assembly, but generally fell between the maximum and minimum measured PCT (central and side rod values, respectively) from experiment. At the midplane, the temperatures leaned towards the maximum value, and at the upper elevations, the temperatures leaned towards the average value. Even with a 1D approximation, TRACE was capable of simulating the trend of PCT transient evolution. An uncertainty analysis using a propagation of input errors (PIE) methodology revealed that for the PIPE component, the most sensitive parameters were the bundle wall emissivity and rod

emissivity, indicating the overall importance of accuracy in the radiation heat transfer model when simulating spray cooling heat transfer. However, the sensitivity analysis of the CHAN component noted that counter-current flow limiting (CCFL) and bundle wall emissivity were the two most influential parameters. This was evident from the results of the CHAN model, where cladding temperatures were over-predicted at the upper axial levels. It was concluded that TRACE likely over-estimated the CCFL phenomenon.

Jaeger and Espinoza [14] applied robust uncertainty quantification using the Software for Uncertainty and Sensitivity Analysis (SUSA) tool developed by Gesellschaft für Anlagen und Reaktorsicherheit (GRS) to a TRACE thermal-hydraulics model (Figure 3) simulating the benchmark LOCA reflooding experiment FEBA (Flooding Experiments with Blocked Arrays). In their analysis, 51 total parameters were identified relating to code uncertainties in the TRACE model input, including 14 material parameters, 27 parameters related to the closure laws for the field equations, and 10 test facility and experimental condition parameters. For these parameters, their ranges of uncertainty were determined through referencing available material or documentation, or estimated by engineering judgment. The TRACE model itself was developed as a single finely-nodalized CHAN component with 43 axial cells to represent the powered assembly, with one FILL component for the flooding inlet (temperature and mass flow rate boundary conditions) and one BREAK outlet component (pressure boundary condition). Using SUSA to generate TRACE model inputs with random perturbations in the 51 parameters, 221 TRACE models were generated corresponding to a statistical fidelity in the output parameter at a double-sided 97.5% confidence level (as determined by Wilks' formula). The output variables quantified in the analysis included cladding temperatures and the time to reflood achieved at three axial positions. The results indicated a typical standard of deviation range of 7.33 – 22.78 K in the peak cladding temperatures and 6.33 - 27.33 sec in the time to reflood, with greater variance towards the top of the bundle. Overall, the

TRACE model was able to predict the trend of PCT, having a tendency to over predict PCT towards the top of the bundle, but showed excellent ability at simulating the time to reflood and progression of the quench front. The 51 input parameters were evaluated by calculating Pearson's correlation coefficient and the associated Pearson partial correlation coefficient to compare their sensitivity to the output parameters. For their TRACE model, it was determined that bundle power had the largest sensitivity across all measured output parameters, with about 15-20 other parameters demonstrating significance (slug flow interfacial friction coefficient and the specific heat of the MgO heater rod bulk material were the most sensitive).

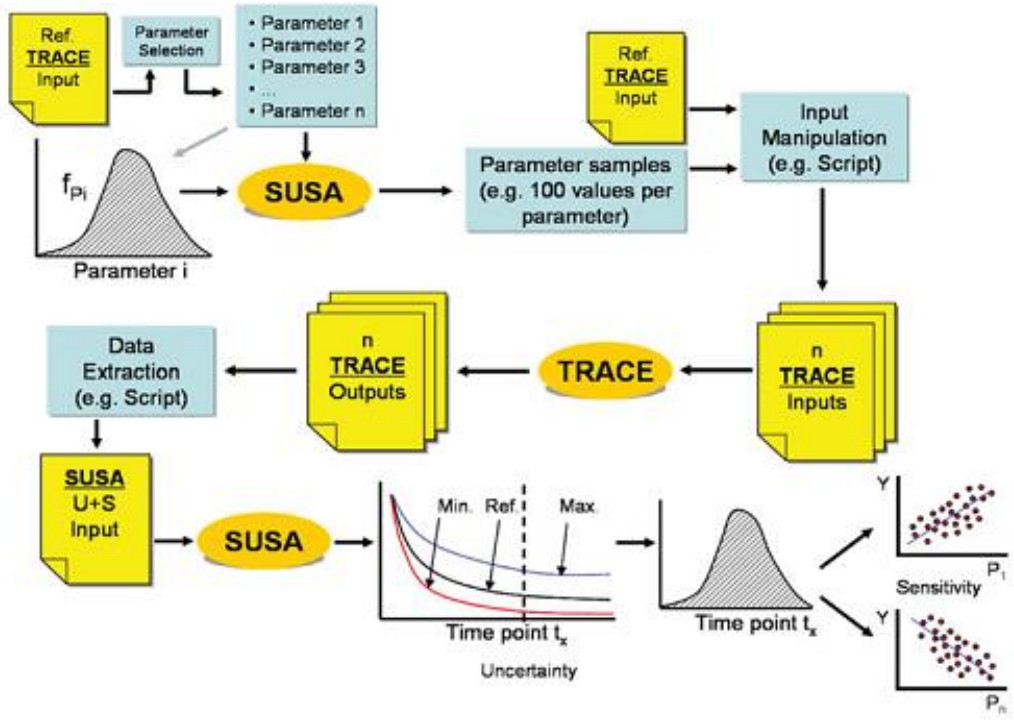

Figure 3. TRACE-SUSA coupling for uncertainty quantification analysis [14].

2. SVEA SPRAY COOLING EXPERIMENT

A test program to evaluate spray cooling performance in a simulated single SVEA-64 fuel assembly was performed in 1986 by ASEA-ATOM as a joint project with the Swedish Nuclear Power Inspectorate and the Swedish State Power Board [15]. The experiment was performed on an evaluation model basis, to obtain heat transfer data of SVEA-64 fuel assemblies under realistic and conservative LOCA conditions. The heat transfer data from this experiment was used to validate the licensing methods applied to SVEA fuel, which are based on the heat transfer coefficients and peak cladding temperatures valid under LOCA conditions [15].

2.1 SVEA Spray Cooling Test Facility

The physical test assembly was built in similar manner to previous single-bundle test facilities, but was primarily concerned with investigation of the interactions between the spray cooling systems and the fuel assembly. The test vessel has an inner diameter of 0.389 m and a height of 5.6m and holds the test bundle. The test vessel is pressurized by a separate large volume pressurizer vessel repurposed from the previous FRIGG experiments (Figure 4). Steam vent lines are incorporated at the top and bottom of the bundle to vary steam venting during the experiment, and are connected to the pressurizer loop. The water drainage system for the test vessel is regulated to maintain the water level in the lower plenum. A coolant injection system is not included in the test vessel, but a bypass flashing water system feeds water into the bypass region of the test section at the bottom of the heated length of the assembly (Figure 5). A separate loop feeds the spray water system from heated storage tanks that are recirculated to maintain constant temperature prior to injection into the test vessel, with a single common fast opening valve to all the spray water lines (Figure 4).

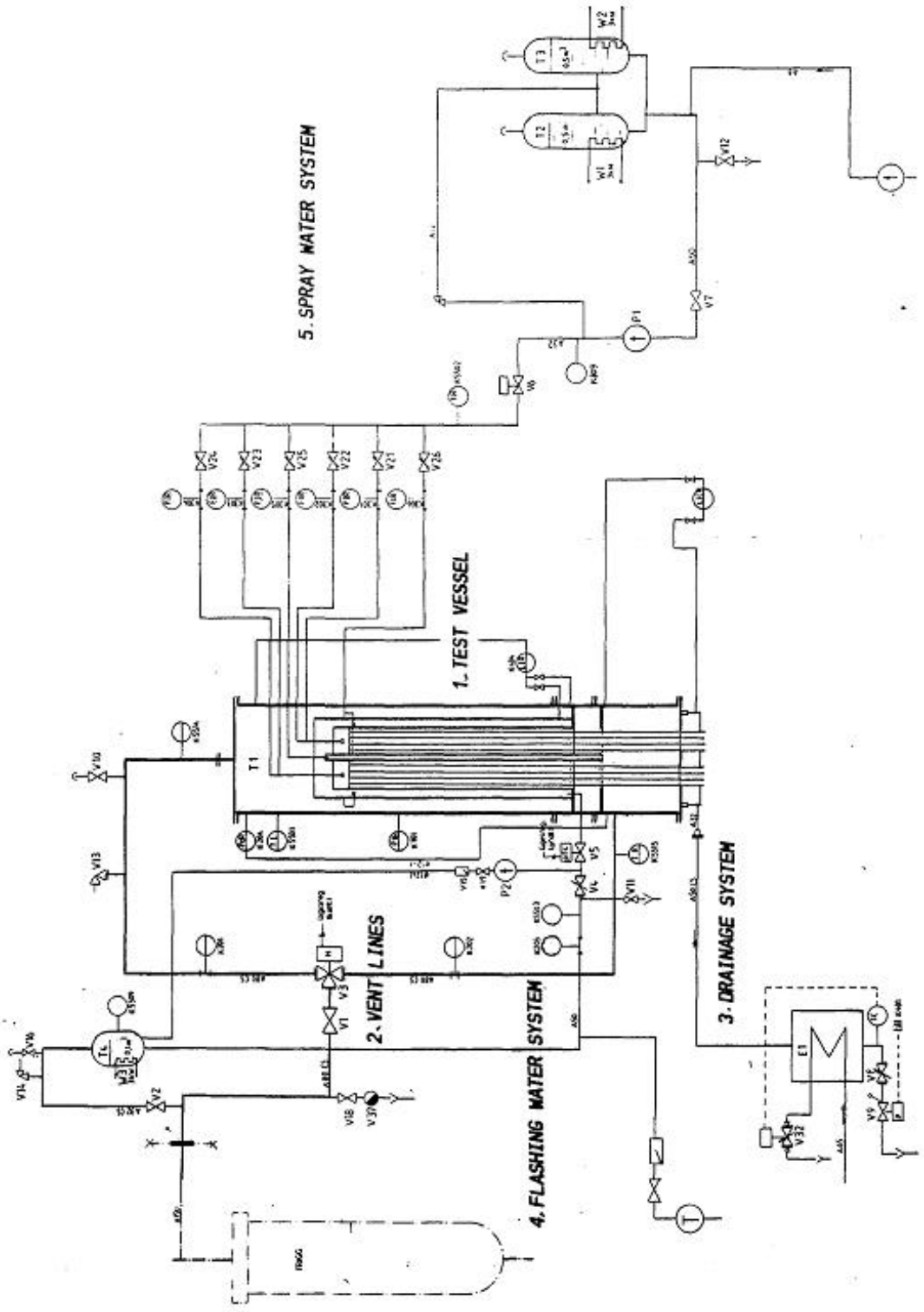

Figure 4. Diagram of test vessel and external systems used in the SVEA spray cooling tests. [2]

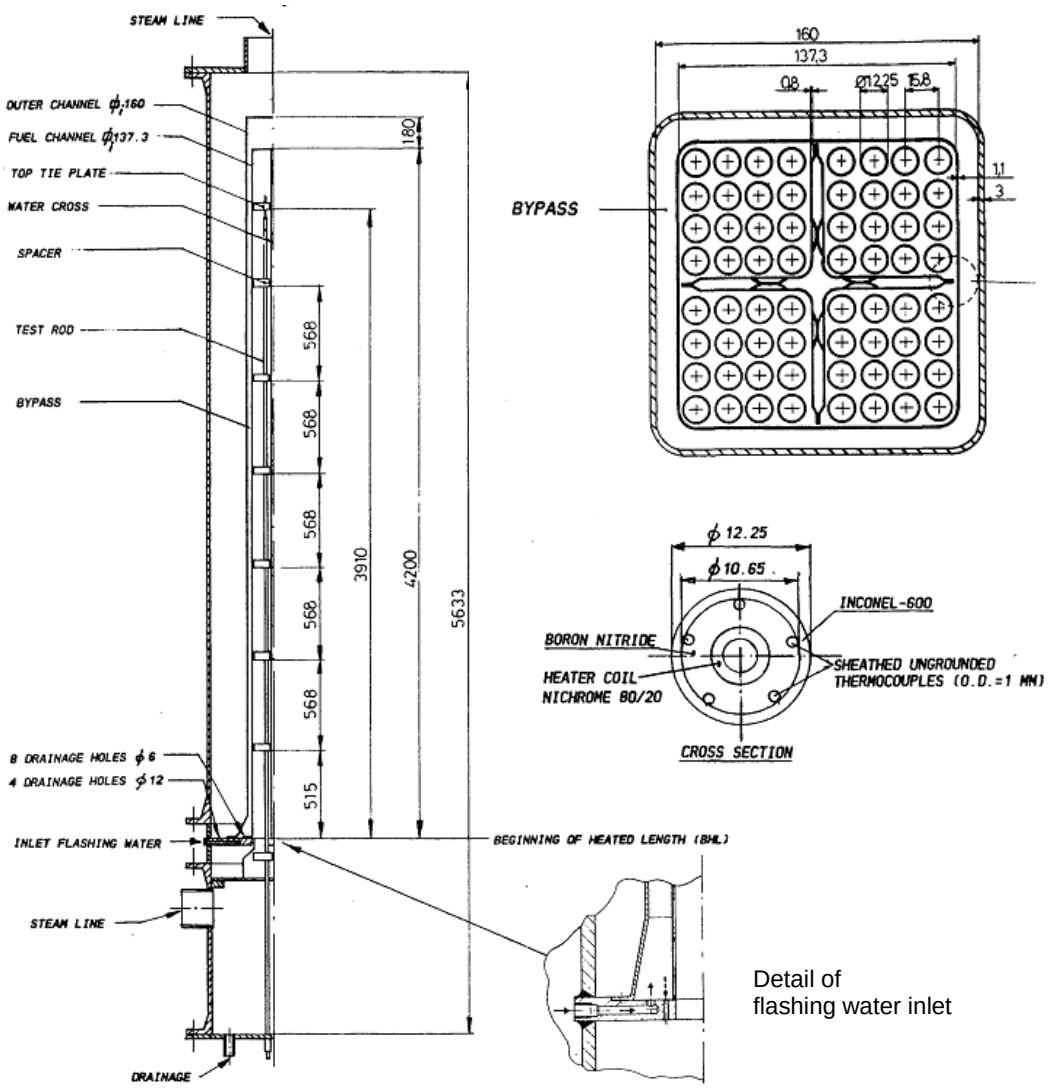

Figure 5. Elevation diagram of the test bundle used in the SVEA spray cooling tests (left), including a cross-section diagram of the representative SVEA-64 assembly (top right) and cross-section of the Inconel-clad nichrome heater rods (right). [2]

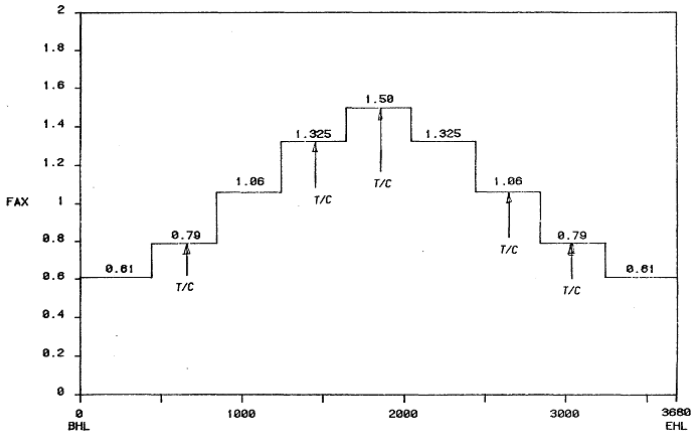

Figure 6. Stepped cosine axial power profile of Inconel heater rods, with thermocouple locations at five axial levels (numbered 1 through 5, from bottom to top of the bundle) [2].

The spray system consisted of 6 individual spray lines: 4 spray nozzles for each sub-bundle of the assembly, one spray water distributor for the water cross, and one line going to four spray distributor units for the bypass region. The sub-bundle nozzles utilized modified LECHLER nozzles that give a 45-50° spray cone angle, with a mounted height 123 mm above the top tie plate. The water cross spray distributor had a 1 mm diameter hole drilled in the center and four 0.5 mm diameter holes along each branch, all pointing downwards. The bypass region spray distributors had four units each with seven holes of 0.5 mm diameter pointing at a 30° angle relative to the vertical plane.

The test bundle itself was designed to fully-represent a standard SVEA-64 fuel bundle (Figure 5) and was constructed of 64 Inconel-clad nichrome coil heater rods equipped with 320 ungrounded Inconel-sheathed type K MgO-insulated thermocouples (establishing 5 axial locations of temperature measurement along each rod, Figure 6), and were arranged in standard SVEA spacers with an upper tie plate slightly modified to accommodate electrical connections and compensate for any bowing of the heater rods [2]. The water cross and fuel channel were constructed of Zircaloy and are also instrumented with thermocouples (32 for the water-cross and 64 for the fuel channel). The outer channel of the fuel bundle was constructed of stainless steel, in order to simulate the bypass region. The power distribution to the heater rods was designed to simulate reactor fuel conditions at roughly 5000 MWd/tU of burn-up with a stepped axial cosine profile (Figure 6). The American Nuclear Society 1979 decay heat curve standard (with +2σ conservatism) with a nominal initial assembly power of 400 kW was chosen for most of the tests performed in the experiment. The total spray water flow to the test bundle was up to 300 g/s, varying in distribution between the sub-bundles, bypass region and water cross.

The data collection system provided relatively good comparison of rod temperatures with measurements for every single rod, but a relatively coarse picture of the axial temperature distribution with 5 axial measurements for each rod. The Table 1 gives an estimated accuracy of the instrumentation used in the test bundle.

Table 1. Accuracy of variables measured in the SVEA spray cooling tests. [2]

Variable	Accuracy	Notes
Absolute pressure	± 0.1 bar	Upper part of test vessel
Spray water flows	± 1%	
Flashing water flow	± 2%	
Steam flows	± 10%	Upper and lower vent lines
Water levels	± 10 cm	Bypass, differential pressure transducers
Test bundle pressure drop	± 1%	Out of range in many tests
Temperatures	± 3° C	Below 300° C
Temperatures	± 0.75% + 1° C	Higher temperatures
Bundle power	± 2.5 KW + 0.2%	
Nominal power distribution	< ± 1%	
Axial power distribution	± 1.5%	Variation in heater coil pitch between rods

2.2 Experiment Procedure

The experiment test procedure is designed to simulate LOCA phenomena that take place from the end of the blowdown phase through the refill-reflood phases, terminating well after fuel rod cladding quench is achieved. The primary phenomenon investigated in this experiment is the propagation of spray water into the core, the subsequent rise in cladding temperature, and the quenching of the fuel rods. In addition, the phenomenon of blowdown flashing (which carries liquid and vapor into the core) is considered in the experiment bundle design and test procedure. Throughout all tests, the vessel was held at a constant system pressure (2 bar). The test vessel has a very limited ‘lower plenum’ region that does not employ a method of realistically simulating the flashing phenomenon of depressurization of the lower plenum leading to two-phase fluid swelling up through the core. Instead, a ‘flashing water’ injection system is included (Figure 5) to simulate the post-dryout cooling that occurs at the end of blowdown. After the vessel reaches a specified

heated state, saturated water is injected at a predetermined flow rate (determined from pre-calculations using the GOBLIN (DRAGON) thermal-hydraulics code) at the bottom of the bundle into the bypass region, filling the bypass channel and flowing over the top of the bypass separator into the heater rod region. The injection terminates and the bypass channel drains completely. This leaves the bypass channel completely wetted at the start of the refill-reflood phase [2]. The heater rods initiate a decay heat power transient profile while spray injections initiate during this flashing water injection period (Table 2).

Table 2. Typical test event progression during SVEA spray cooling tests [2].

Time (sec)	Event
0	Start logging data
120	System controls manually powered on
191	Pre-calculated vessel break-in time
198	Start injection of flashing water
199	Initiate decay heat power transient
213	Start injection of spray water
218	Stop flashing water injection (end of blowdown phase)
230	Venting direction transitions from lower to upper plenum
1500	System controls manually powered off
1800	Stop logging data

2.3 Test 012 and Test 015

The two tests chosen for comparison in the present work were Test 012 [16] and Test 015 [17], which are representative cases for SVEA reflooding under uniform and non-uniform distribution of spray flow conditions. These tests were considered as the typical scenarios that would be expected in a LOCA scenario, and were two of the three cases used to determine the requirements licensing of spray cooling for SVEA fuel designs for operation in Swedish BWRs [15]. Each experiment demonstrated that even under varying spray flow conditions, the rated design of the spray cooling apparatus and the inherent safety features of the SVEA fuel design were capable of maintaining safe core conditions

throughout a LOCA, particularly through the simulated refill-reflood phase. The peak cladding temperatures measured in both tests were similar despite the difference in spray cooling distribution, with the rest of the experimental parameters kept as nominally consistent.

Table 3.Experimental parameters for SVEA Spray Cooling tests 012 and 015 [16] [17].

Parameter	Test 012	Test 015
Date of test	05-07-1986	05-13-1986
System pressure (bar)	2	2
Initial Bundle Power (KW)	379	406
Decay Power	ANS-79 + 2σ	ANS-79 + 2σ
Sub-bundle 1 spray flow (g/s)	40	80
Sub-bundle 2 spray flow (g/s)	40	55
Sub-bundle 3 spray flow (g/s)	40	55
Sub-bundle 4 spray flow (g/s)	40	35
Water cross spray flow (g/s)	10	10
Bypass spray flow (g/s)	130	65
Peak Cladding Temperature	1003	994

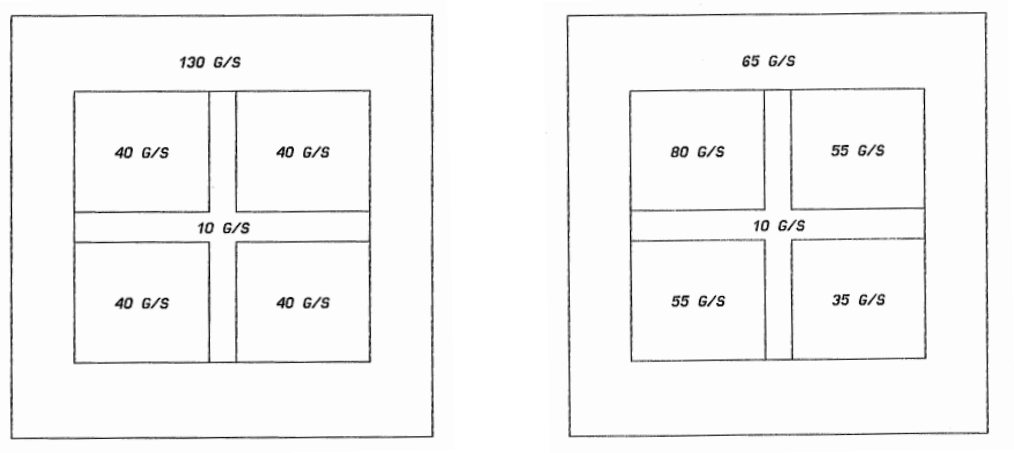

Figure 7. Diagram of spray flow distribution across the sub-bundle, water cross and bypass channels for Test 012 (left) and Test 015 (right). Total spray flow to the test bundle was maintained at 300 g/s [2].

3. TRACE AND DAKOTA COMPUTATIONAL MODEL

The SVEA spray cooling experiment is modeled with a best-estimate plus uncertainty approach by using available codes suitable for this methodology. The thermal-hydraulics modeling is developed using the US NRC-supported code TRACE version 5.0 Patch 4. The uncertainty quantification implemented on the TRACE model is performed using Dakota version 6.2 (Design Analysis Kit for Optimization and Terascale Applications), an open-source software developed by Sandia National Laboratories. The entire computational model is developed using the Symbolic Nuclear Analysis Package (SNAP) framework to generate the model inputs for both TRACE and Dakota, as well as handling the tasks of code execution and monitoring.

3.1 TRACE Capabilities

The most recent efforts by the US NRC in best-estimate computational modeling of nuclear reactor performance has been incorporating the NRC's four main systems codes (TRAC-P, TRAC-B, RELAP5 and RAMONA) into the TRAC/RELAP Advanced Computational Engine (TRACE) [18]. Developed for light-water reactors, TRACE is a system code that utilizes a component approach to modeling the reactor system, which are divided into a finite number of cells. TRACE is built on the two-fluid six-equation two-phase flow model that solves the conservation equations for mass, momentum and energy for the separate liquid and vapor phases of water with a common pressure field. For non-condensable phases in vapor, mixture equations for the conservation of momentum and energy are utilized. For these conservation equations, additional closure laws and constitutive relations are required to obtain a complete solution, which results in ten parameters that must be modeled: interfacial area, interfacial mass transfer, interfacial drag, liquid and vapor wall drag, liquid and vapor interfacial heat transfer, liquid-to-vapor

sensible heat transfer coefficient, and the liquid and vapor wall heat transfer coefficients. The computational approach to solve for each cell uses several numerical schemes [18]:

1. Partial differential equations for two-phase flow and heat transfer are solved by a finite volume scheme.
2. Heat transfer equations are solved by semi-implicit time-differencing scheme
3. Fluid dynamics considered in individual components use multistep time-differencing schemes (SETS) or semi-implicit time differencing schemes.
4. The nonlinear equations for hydrodynamic phenomena are coupled using finite difference scheme and solved by Newton-Raphson iteration scheme.
5. Subsequent linearized equations are solved directly.

TRACE considers several different two-phase flow regimes to solve the heat transfer and drag models, and has two sets of selection criteria depending on conditions in relation to the critical heat flux (CHF). In the present case, the experiment simulates reflood which occurs post-CHF, for which TRACE determines flow regime based on wall temperature and void fraction (Figure 8) [18].

The PIPE, CHAN (BWR fuel channel) and VESSEL (reactor vessel) components comprise the hydraulic volume models that are typically used for the core region. HTSTR (heat structure) and RADENC (radiation enclosure) components further define hydraulic components to incorporate energy transfer into the fluid models. TRACE does not have a specific component to simulate spray cooling injection, as the flow regime in PIPE and CHAN components are approximated as 1D (fluid injection is modeled with a FILL component). Particularly for BWR LOCA, some special models and options are necessary to activate in TRACE to increase the accuracy of modeling specific phenomena.

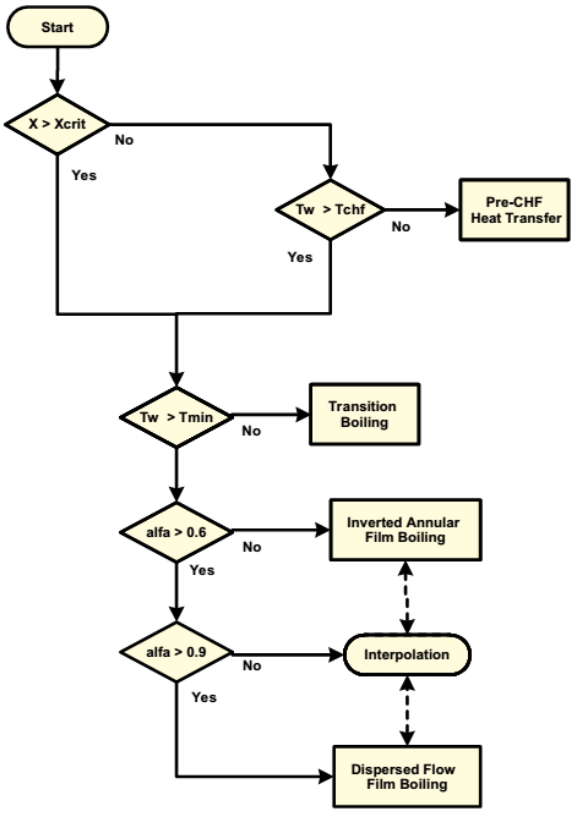

Figure 8. TRACE selection logic for determination of two-phase flow regime in post-CHF conditions [18].

TRACE is able to dynamically adjust the nodalization of components to capture small-scale phenomena. The fine mesh reflood option dynamically adds and removes HTSTR axial nodes during calculation, and an option for axial heat conduction is also available to model the quench front with greater accuracy than a radial-only conduction model. The radiation model in TRACE also differs depending on the bundle component type selected (PIPE vs. CHAN). Both models require input for the surface emissivity, view factor and beam lengths. The CHAN component has an option to automatically evaluate the view factors and beam lengths through a Monte Carlo simulation. TRACE also includes a CCFL model that can be activated in specific locations where CCFL is expected to occur. The CCFL model incorporates and selects between three correlations: Wallis, Kutateladze, and Bankoff and the selection criteria is specified by the user in the input.

3.2 TRACE Model of SVEA Spray Cooling Experiment

The TRACE model developed in this work focuses on representing the test bundle in the experiment, adding components as needed to represent the rest of the test loop facility (Figure 9). The PIPE component was chosen to simulate the four bundle sub-channels, the bypass channel and the water cross channel. Four HTSTR components (HTSTR) simulate the four groups of 4 x 4 heater rods in each sub-bundle. Four HTSTR components are also used to simulate the heat transfer coupling of each sub-bundle to the bypass channel, as well as an additional four HTSTR components that simulate the heat transfer coupling of each sub-bundle to the water cross channel. One HTSTR component simulates the outer channel wall and is coupled to the bypass channel. For each channel, TEE components are used to simulate portion of the upper and lower plenums in the test vessel. FILL components are used to simulate the spray coolant injection for each of the six channels (which have different flow rates, depending on the experiment), and are controlled by a TRIP block that initiates spray cooling at the desired time. The upper and lower plenums both have a BREAK component connected to VALVE component that simulates the steam vents, and are controlled by a TRIP block that initiates the transition of steam venting from one to the other at a given time according to the experiment test parameters. Each lower plenum TEE component is also connected to a BREAK and VALVE component that simulates the water drain, and is controlled by a TRIP block that is defined by the void fraction at the BREAK. For the bypass channel, a FILL and VALVE component is connected at the base of the bypass PIPE component to simulate the flashing water injection portion of the experiment. The VALVE closes to allow coolant to be injected at a specified rate from the FILL component into the bypass channel PIPE component, and then opens according to the experiment time, shortly after spray cooling injection is initiated.

In addition to these basic hydraulic components, several code options and models are activated to improve the accuracy of the simulation. A radiation model is defined for each sub-channel to simulate radiation heat transfer from the heater rod HTSTR component in each sub-bundle to their respective HTSTR components simulating the bypass channel and water cross channel. In this work, the entire 4 x 4 sub-bundle is treated as a single radiation group, and average values are taken for the view factors (A.1). Since TRACE uses a 1-D calculation, the radial distribution of temperature between individual heater rods across the bundle is not modeled. The fine mesh reflood option and axial heat conduction models were utilized in this TRACE model, and significantly improved the temperature prediction across all axial levels. The fine mesh reflood option divides the 9 axial cells dynamically (re-nodalizing each cell into an up to additional 3 cells) to obtain a more accurate axial temperature profile, but also significantly increases the computational time required for each model run (from a few minutes to over two hours increase in computational time). A counter-current flow limiting (CCFL) model was also implemented in the sub-channel PIPE components, and utilizes the Bankoff model, which interpolates between the Wallis and Kutateladze models (Table 4). For the present TRACE model, the Wallis model was selected since previous work has shown that this model is preferable for relatively small hydraulic diameters (2.5 to 50 mm), relevant to the present case [19].

Table 4. Comparison between countercurrent flow limit correlation modes incorporated in TRACE [18].

Correlation	Parameter	Geometry	Location
Wallis	Dimensionless superficial velocity	Small diameter tubes/holes	Fuel channel
Kutateladze	Kutateladze number	Large hole diameters, large perforation ratios and thin plates	Fuel channel
Bankoff	Interpolates Wallis and Kutateladze	Small hole diameters, small perforation rations, thick plates	Upper tie plate

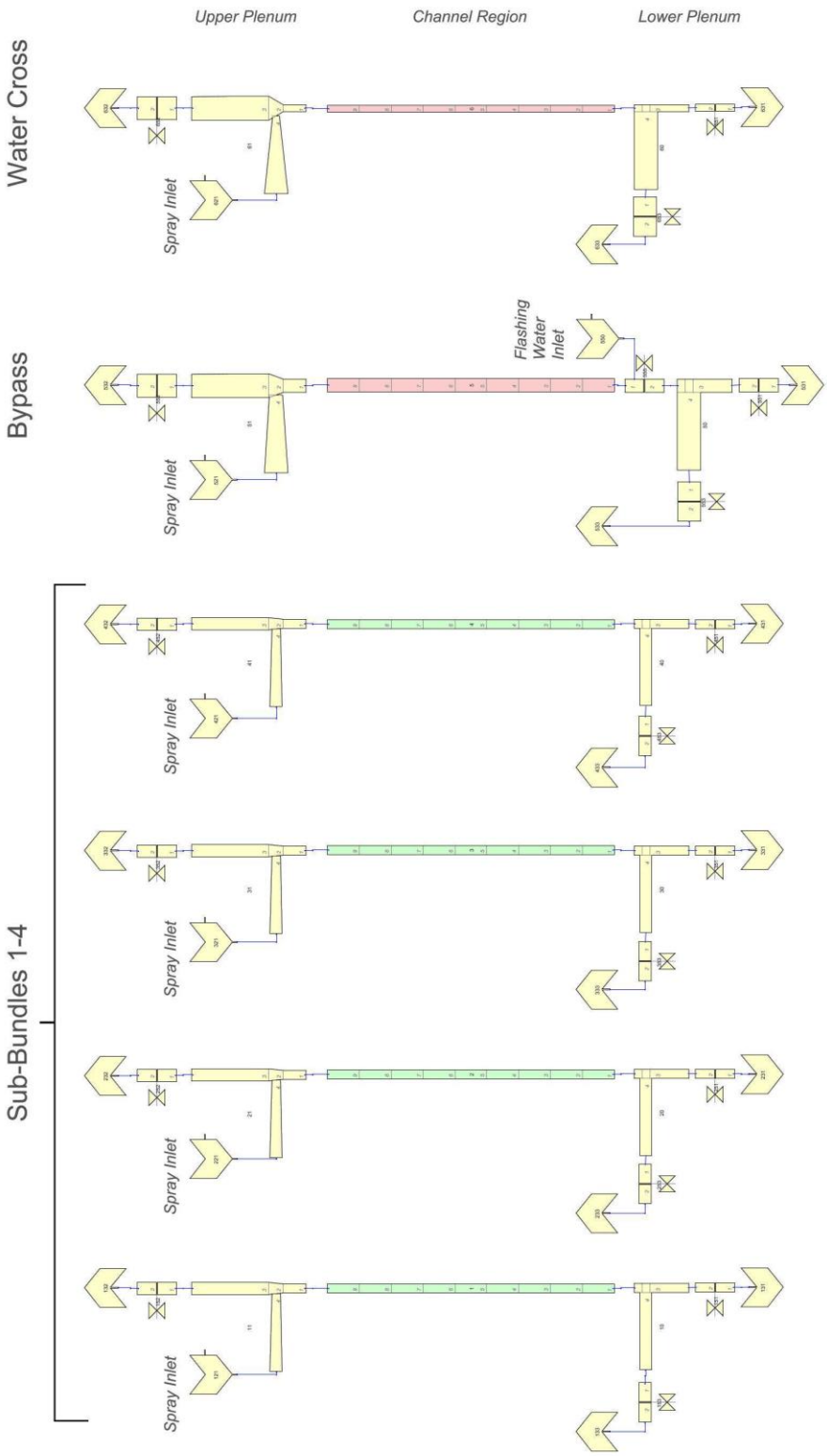

Figure 9. TRACE model developed to simulate the SVEA spray cooling experiments. The main hydraulic components are represented in this diagram.

3.3 Dakota Uncertainty Quantification Analysis and Configuration

The Dakota (Design Analysis Kit of Optimization and Terascale Application) software [20] was developed by Sandia National Laboratories initially as a common set of optimization tools used by engineers for structural analysis. Out of a need for a common interface to utilize these frequently used optimization tools, Dakota was developed as a flexible means of interfacing analysis methods to virtually any simulation code. For sensitivity analysis and parameter sampling, Dakota is able to loosely couple with a "black-box" simulation code by measuring the response between a set of user-defined input parameters and one or more output parameters of interest from the simulation code being analyzed. Particularly for TRACE, there is a well-developed interface between Dakota and TRACE for uncertainty analysis, with the ability to develop code inputs and manage execution through the SNAP interface. In this method, forward uncertainty quantification is performed by propagating the specified TRACE model input uncertainties through the code and measuring the response on an output parameter (e.g. the peak cladding temperature). For the developed SVEA spray cooling experiment TRACE model, 31 total sensitivity parameters (Table 5) were identified and described. Parameters 1-8 describe uncertainty in the thermal-hydraulics boundary conditions of the model; their uncertainty quantities were found in the original documentation of the experiments from Asea-Atom [2]. Parameters 9-14 describe uncertainties in the vessel geometry, and parameters 15-24 pertain to uncertainties in the bundle geometry and physical model parameters (radiation and CCFL). Parameters 25-28 are sensitivity coefficients of constitutive models used by TRACE to determine heat transfer in different flow regimes. TRACE allows these coefficients to be multiplied by a constant factor defined in the input model, 1.0 being the nominal value for the base (unperturbed) simulation. Parameters 29-31 are the interfacial and wall drag coefficients used by TRACE. Parameter uncertainties and selection criteria are discussed in Appendix B.

Table 5. Uncertainty quantification parameters considered from TRACE input model and physical models.

Number	Parameter	Uncertainty	Reference Value	Distribution	Reference
Thermal Hydraulic Initial Parameters					
1	Spray system pressure	0.1 bar	2 bar	Uniform	[2] pg. 16
2	Spray system temperature	0.75%	323 K	Uniform	[2] pg. 17
3	Bundle spray mass flow	1%	20-80 g/s	Uniform	[2] pg. 16
4	Bypass spray mass flow	1%	65-130 g/s	Uniform	[2] pg. 16
5	Water cross spray mass flow	1%	10 g/s	Uniform	[2] pg. 16
6	Water drain temperature	0.75%	323 K	Uniform	[2] pg. 17
7	Steam vent temperature	0.75%	393 K	Uniform	[2] pg. 17
8	Outlet pressure	0.1 bar	2 bar	Uniform	[2] pg. 16
Vessel-related parameters					
9	Bundle wall roughness	30%	1×10^{-6} m	Normal	[21] pg. 3.32
10	Bypass channel wall roughness	30%	1×10^{-6} m	Normal	[21] pg. 3.32
11	Water-cross wall roughness	30%	1×10^{-6} m	Normal	[21] pg. 3.32
12	Length of main channel	0.01 m	3.68 m	Uniform	Appendix B
13	Length of bypass channel	0.01 m	3.68 m	Uniform	Appendix B
14	Length of water-cross	0.01 m	3.68 m	Uniform	Appendix B
Bundle-related parameters					
15	Bundle flow area	1.00%	2.428×10^{-3} m^2	Uniform	[22] pg. 14
16	Bundle hydraulic diameter	1.00%	0.01114 m	Uniform	[23] pg. 21
17	Bypass channel flow area	1.00%	6.14×10^{-3} m^2	Uniform	[22] pg. 14
18	Bypass hydraulic diameter	1.00%	0.0884 m	Uniform	[23] pg. 21
19	Water Cross flow area	1.00%	1.612×10^{-3} m^2	Uniform	[22] pg. 14
20	Water Cross hydraulic diameter	1.00%	0.0453 m	Uniform	[23] pg. 21
21	Rod emissivity	0.10	0.45	Uniform	[2] pg. 17
22	Bundle wall emissivity	0.10	0.3	Uniform	[2] pg. 17
23	CCFL slope	0.8-1.0	1.0	Uniform	[24] Ch. 11
24	CCFL constant	0.88-1.0	1.0	Uniform	[24] Ch. 11
Heat Transfer Coefficients (TRACE Code physical models)					
25	DFFB Wall-Liq. HTC	45%	1.0	Uniform	[25] pg. 149
26	Wall Liquid HTC	15%	1.0	Uniform	[26] pg. 2373
27	Wall Vapor HTC	20%	1.0	Uniform	[27] pg. 59
28	DNB/CHF	8%	1.0	Uniform	[28] pg. 10
Interfacial Drag Coefficients (TRACE Code physical models)					
29	Annular-Mist Interfacial Drag	25%	1.0	Uniform	[24] Fig. 11-3
30	DFFB Interfacial Drag	40%	1.0	Uniform	[29] pg. 101
31	Wall Drag	5%	1.0	Uniform	[30] pg. 514

Dakota modifies a reference TRACE input model, and is able to use any parameter that is user-defined in the TRACE model as an uncertainty input (Figure 10). In Dakota, each input parameter (uncertainty parameters) require probability distributions which Dakota will sample. In this work, almost all of the input parameters were defined with a uniform distribution, since no prior information was known about the distribution of each parameter (except for wall roughness [21]). A uniform distribution was chosen as to not bias the uncertainty quantification results a-priori, with the intent that in a random sampling of these parameters, any extreme case is as likely as the reference values. Dakota randomly samples these parameters from the defined distributions through a Monte Carlo sampling routine. From the TRACE model, an ExtractData script takes the output data file and stores the peak cladding temperature for all four sub-bundles. This output parameter is strictly a scalar quantity; it does not consider the transient evolution of the PCT, though it is possible in Dakota to define more than one output parameter for uncertainty evaluation.

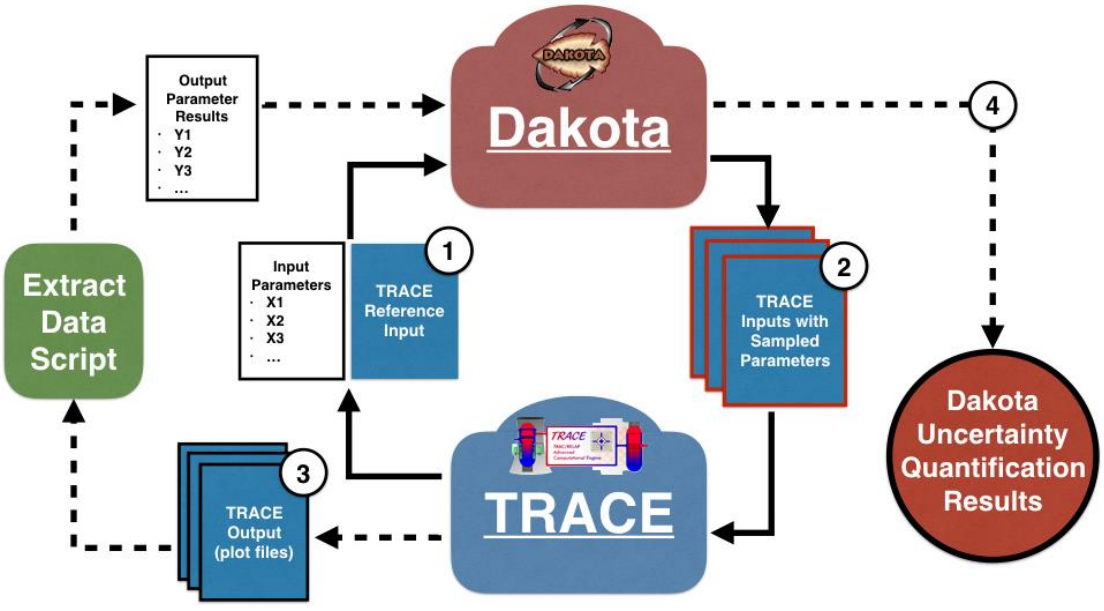

Figure 10. Uncertainty quantification schematic of coupling between TRACE and Dakota in SNAP.

The number of required simulation code calculations is defined by Wilks's formula [31] (equation 1):

$$1-\left(\frac{\alpha}{100}\right)^{N} \geq \frac{\beta}{100} \tag{1}$$

Wilks's formula states for *N* calculations, the combined propagated uncertainties of a sample will yield least *α* % of the samples that lie below the tolerance limit with *β* % confidence. For two-sided statistical tolerance limits, Wilks's formula is also given as:

$$1-\left(\frac{\alpha}{100}\right)^{N} - N\left[1-\left(\frac{\alpha}{100}\right)\right]\left(\frac{\alpha}{100}\right)^{N-1} \geq \frac{\beta}{100} \tag{2}$$

For the uncertainty quantification of this TRACE model, a 95% double-sided confidence interval was chosen, with Wilks's formula (equation 2) indicating that at least 93 simulation code calculations are required.

Dakota uses two statistical methods to quantify the sensitivity of the output parameter to the input parameters. The Pearson correlation determines the level to which two parameters (*x* and *y*, for example) correlate in a linear manner. This correlation (*r*) is determined from the covariance (equation 3) [20]:

$$r = \frac{\sum_{i=1}^{N}\left(x_i-\mu_i\right)\left(y_i-\mu_i\right)}{\left[\sum_{i=1}^{N}\left(x_i-\mu_i\right)^2\sum_{i=1}^{N}\left(y_i-\mu_i\right)^2\right]^{1/2}} \tag{3}$$

However, if the relationship between the two parameters is non-linear (e.g. polynomial, exponential, etc.), the covariance is dependent on the scale of the two parameters and may not be able to determine the strength of the correlation due to the large discrepancy, therefore the covariance is divided by the standard deviations (equation 3). In the case that one or more of the parameters are not quantitative or interval quantities, but rather are described by ordinal rank-type quantities, a non-parametric correlation must be used.

Dakota also computes the Spearman's rank correlation coefficient by replacing all of the parametric raw data with rank values (tied ranks receive an averaged rank value). Spearman's rank correlation (ρ) is determined by the differences $d_i = x_i - y_i$ between the parameter ranks (equation 4) [20]:

$$\rho = 1 - \frac{6\sum_{i=1}^{N} d_i^2}{n\left(n^2 - 1\right)} \tag{4}$$

In this way, Spearman's correlation determines the monotonic relationship between two parameters. Dakota also calculates the partial correlation coefficients for both Pearson's coefficient and Spearman's coefficients. This is useful in the case where multiple input parameters are being perturbed simultaneously, which may result in one input parameter influencing another input parameter in an unexpected manner that results in an unconsidered bias on the output parameter.

4. RESULTS

In the SVEA spray cooling experiments, the test bundle is instrumented to record cladding temperatures for every single heater rod at 5 common axial locations across the entire bundle. As a result, the experimental data records a range of cladding temperatures at each axial level, strongly dependent on their radial location and proximity to the sub-bundle channel walls. In the experiment, it was frequently observed that spray water injected into the sub-bundle typically flows downward in the periphery of the sub-bundle, while upward-flowing vapor tends to occupy the central region of the sub-bundle [15]. Furthermore, the separate spray flow injection into the bypass channel and water cross results in those components acting as heatsinks which promoted increased radiation heat transfer from the peripheral heater rods due to their proximity [2]. As a result, the range of cladding temperature at each axial level is often large. TRACE does not capture the radial distribution of cladding temperatures, as component geometry uses a 1-D calculation methodology and each 4 x 4 sub-bundle is represented by a single HTSTR heat structure component representing an averaged heater rod.

However, TRACE is generally able to simulate the cladding temperatures within the range of the experimental data. In the case of uniform spray flow between the sub-bundles (Test 012 [16]), TRACE is able to model the average cladding temperatures fairly well for the middle of the bundle, but does not perform as well for the top and bottom of the bundle. At axial level 1 (the bottom of the bundle), TRACE over predicts the cooling that occurs, and quenches much earlier than experimental measurement. The opposite trend occurs at the top of the bundle, where TRACE predicts the quenching to occur much later than the experimental measurement, with peak cladding temperature under-predicted at the top of the bundle.

Test 012 – Uniform Spray Flow Conditions (40 g/s)

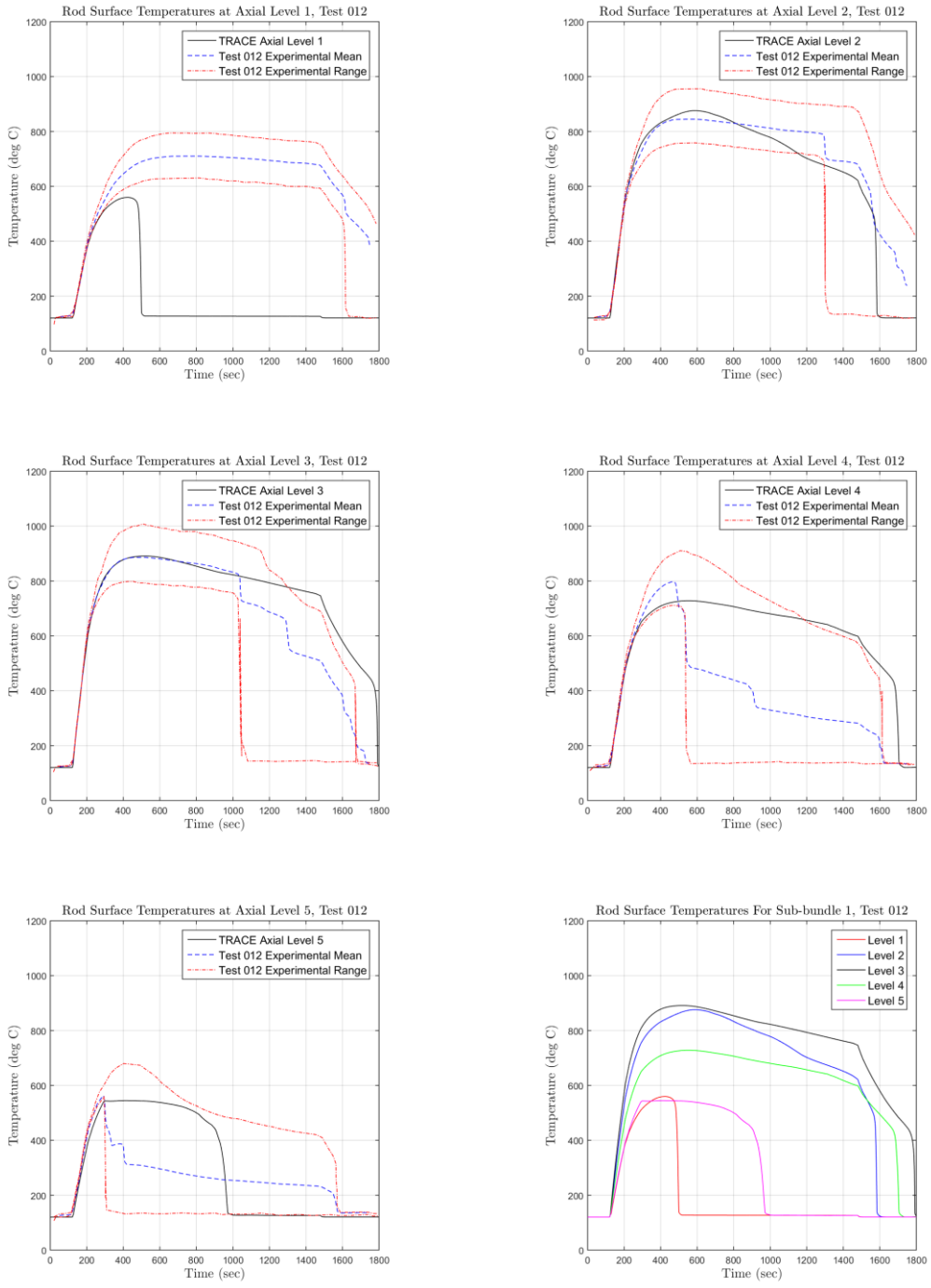

Figure 11. Comparison of TRACE peak cladding temperatures to the measured experimental data range from SVEA spray cooling Test 012 which exhibited a uniform 40 g/s spray cooling to each sub-bundle. Comparisons are made at 5 axial locations, from the bottom of the bundle at level 1 (top left) up to the top of the bundle at level 5 (bottom left). All axial TRACE predictions are compared together (bottom right).

Test 015 – Non-uniform Spray Flow Conditions, Sub-Bundle 1 (80 g/s)

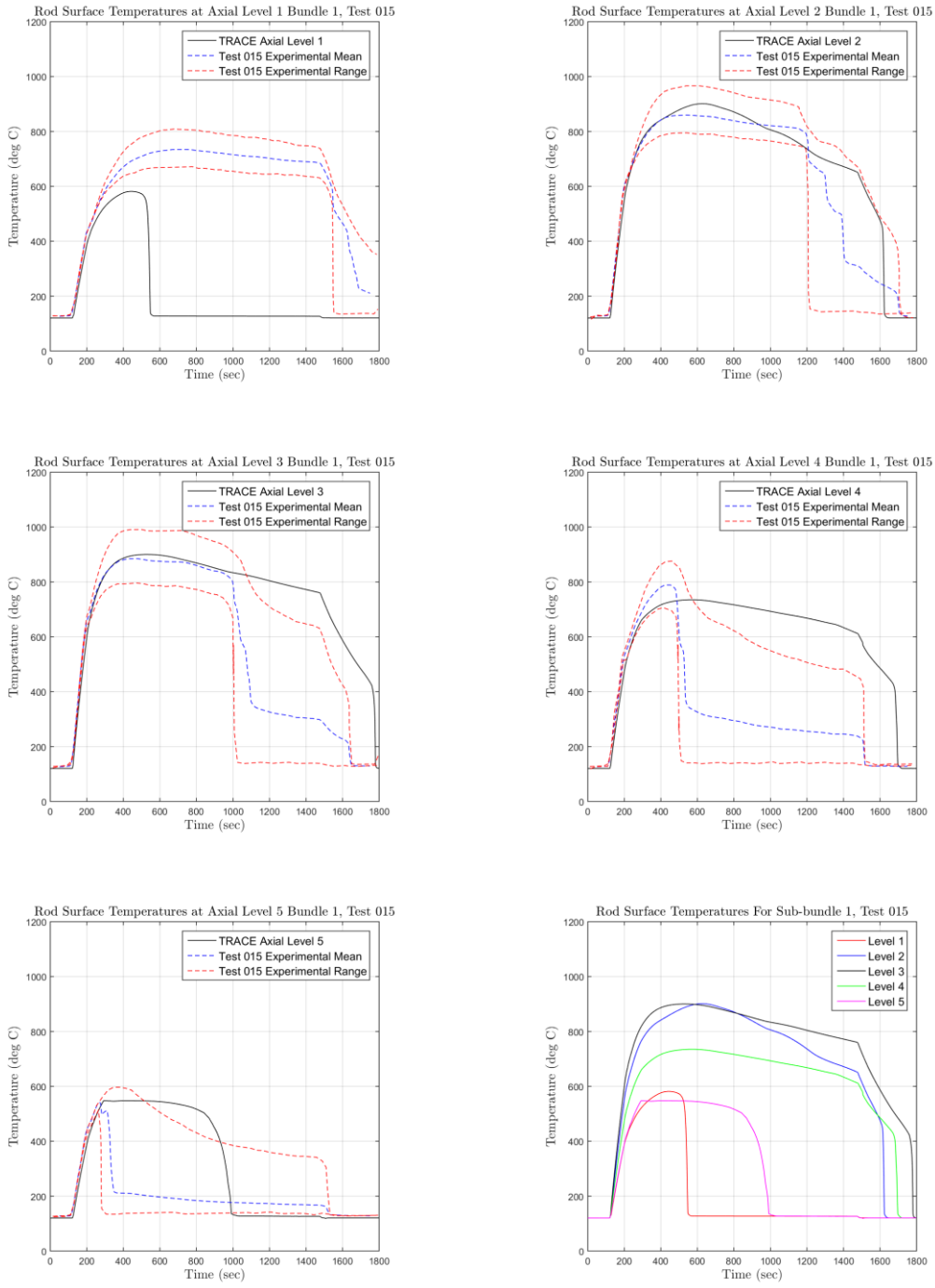

Figure 12. Comparison of TRACE peak cladding temperatures to the measured experimental data range from SVEA spray cooling Test 015 for sub-bundle 1 (receiving 80 g/s spray flow). Comparisons are made at 5 axial locations, from the bottom of the bundle at level 1 (top left) up to the top of the bundle at level 5 (bottom left). All axial TRACE predictions are compared (bottom right).

Test 015 – Non-uniform Spray Flow Conditions, Sub-Bundle 2/3 (55 g/s)

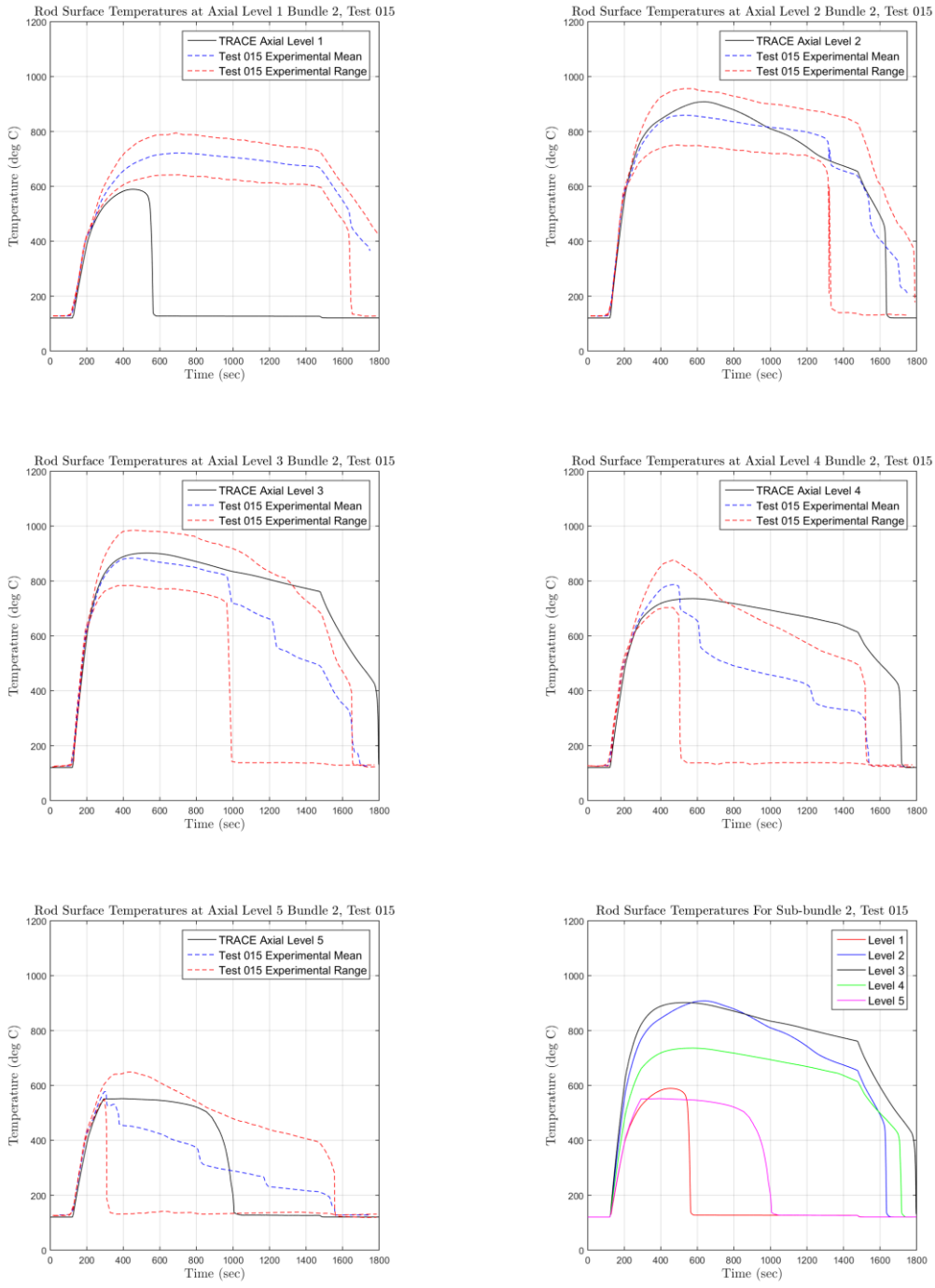

Figure 13. Comparison of TRACE peak cladding temperatures to the measured experimental data range from SVEA spray cooling Test 015 for sub-bundle 2 (receiving 55 g/s spray flow). Comparisons are made at 5 axial locations, from the bottom of the bundle at level 1 (top left) up to the top of the bundle at level 5 (bottom left). All axial TRACE predictions are compared (bottom right).

Test 015 – Non-uniform Spray Flow Conditions, Sub-Bundle 4 (35 g/s)

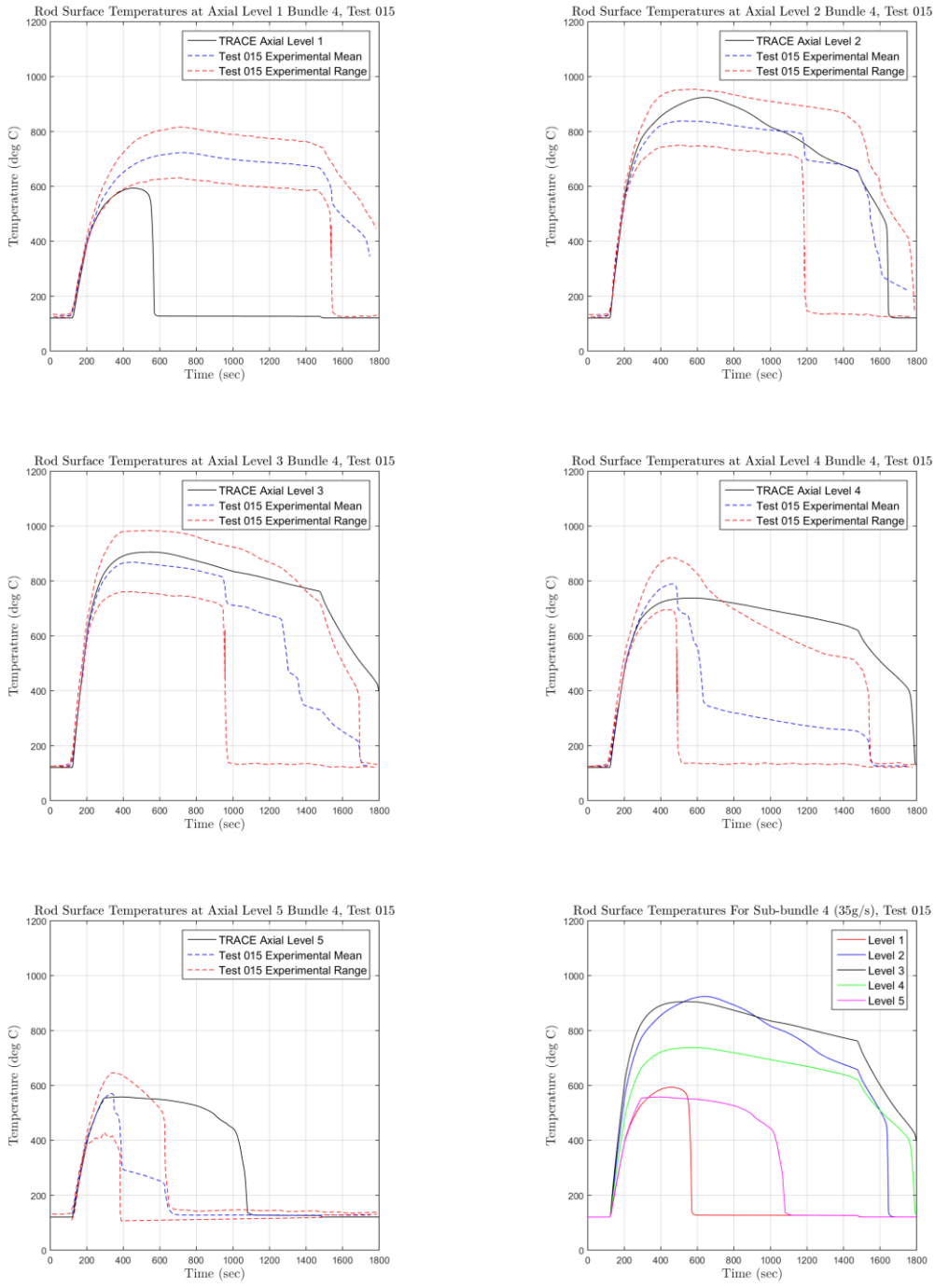

Figure 14. Comparison of TRACE peak cladding temperatures to the measured experimental data range from SVEA spray cooling Test 015 for sub-bundle 4 (receiving 35 g/s spray flow). Comparisons are made at 5 axial locations, from the bottom of the bundle at level 1 (top left) up to the top of the bundle at level 5 (bottom left). All axial TRACE predictions are compared (bottom right).

In the case of non-uniform spray flow between the sub-bundles (Test 015 [17]), TRACE prediction performs similarly to the uniform spray flow case, with relatively good prediction for the axial mid-plane levels of the bundle. (Figure 12 - Figure 14). With the exception of the bottom of the bundle where TRACE over-predicts cooling, the model is able to capture the PCT over the length of the bundle when compared to the experimental mean at each axial measurement. However, TRACE does not predict the onset of quenching as accurately, with a tendency to under-predict quench progression. Additionally, the total spray cooling injection into the sub-bundles is larger in this test (Test 015) relative to the uniform flow test (Test 012) by about 65 g/s. The increased spray flow is compensated by decreased flow into the bypass channel. In comparison between the different sub-bundles, TRACE does not exhibit as much difference between cladding temperature prediction as that of the experimental data. In the test setup, it was suggested that cross-flow between bundles (across gaps in the edge of the water cross) allowed for some fluid interaction between bundles, but it is not very feasible to represent this phenomena in the 1-D modeling of TRACE. The most significant differences in TRACE results across sub-bundles occurs towards the end of the transient, suggesting that in the TRACE model the dominant heat transfer mode is through radiation which is relatively consistent across all 4 sub-bundles and less sensitive to the difference in spray flow rate. In the experiment, there may be other fluid flow phenomena such as CCFL that are not fully represented in TRACE. Nonetheless, the trend of the cladding temperature is captured correctly by TRACE.

For the Dakota uncertainty model, the TRACE model for Test 012 and Test 015 was randomly sampled over the 54 input parameters of interest (see Table 5). In both cases, the mean and median values of the peak cladding temperature over 100 sampled cases lie in the experimental data range. The transient peak cladding temperature (including all four sub-bundles) from all 100 sampled cases was plotted along with the base TRACE

model prediction and the experimental range for comparison (Figure 17, Figure 18). The uncertainty model demonstrates that TRACE is able to predict the range of peak cladding temperatures measured from the experiment. For the uncertainty analysis of Test 015, a consistency argument was included to verify that the peak cladding temperature recorded always occurred in the sub-bundle that received the lowest spray flow (sub-bundle 4). This result confirms that in the TRACE model, the change in peak cladding temperature prediction was only dependent on the change in spray flow distribution from the uniform case in Test 012 to the non-uniform case in Test 015. The overall results of the uncertainty analysis also indicate that forward propagation of the input parameter uncertainties will lead to the present TRACE model over-predicting the peak cladding temperatures, which yields a moderate level of conservatism in the simulation model. Particularly, some of the more extreme cases with higher PCT also exhibit delayed quenching times, a phenomenon which may have an impact on LOCA safety in relation to other material-related phenomena that affect fuel cladding integrity.

Table 6. Comparison of Dakota uncertainty results for 100 sampled cases of the TRACE model.

Source	Result	Test 012 Peak Cladding Temperature (°C)	Test 015 Peak Cladding Temperature (°C)
Uncertainty Quantification cases (100 samples)	Min Value	869.65	881.11
	Max Value	1067.94	1109.48
	Mean	959.37	998.17
	Median	962.05	1001.72
	Standard Deviation	50.08	59.42
Reference TRACE Model (Unperturbed)	--	890.99	905.39
Experiment Data from Test 012 (axial level 3) [16] and Test 015 (sub-bundle 4, Axial level 3) [17]	Min Value	711.21	761.75
	Max Value	1007.38	983.87
	Mean	886.69	868.41

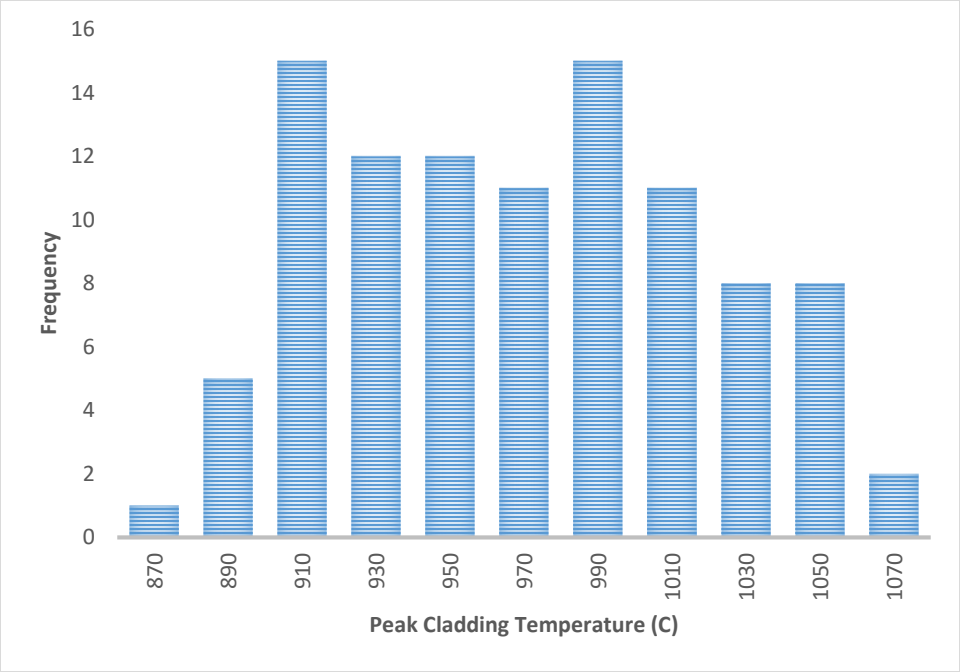

Figure 15. Distribution of peak cladding temperatures from 100 uncertainty quantification calculations of the TRACE model for Test 012 randomly sampled on 31 parameters.

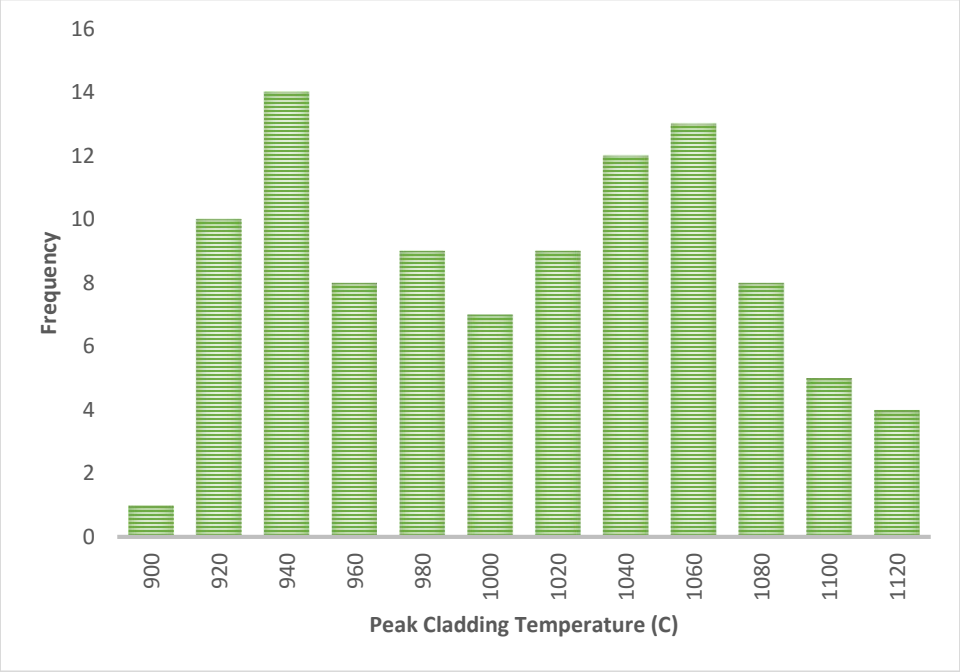

Figure 16. Distribution of peak cladding temperatures from 100 uncertainty quantification calculations of the TRACE model for Test 015 randomly sampled on 31 parameters.

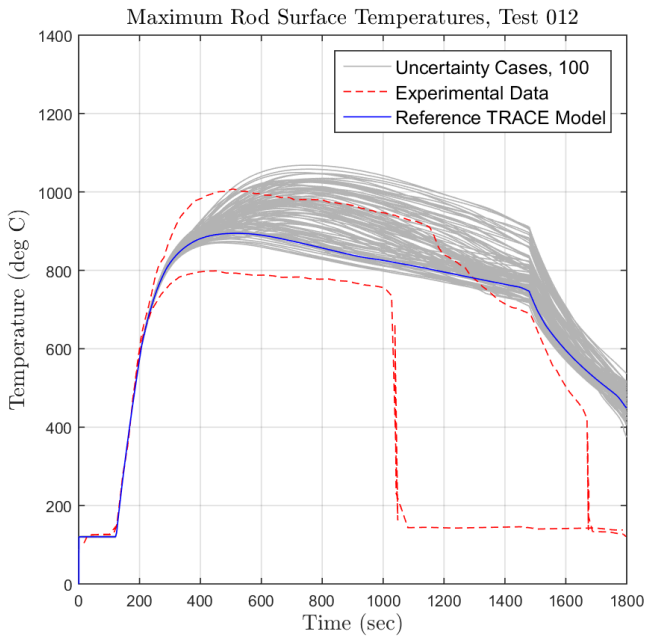

Figure 17. Peak cladding temperatures for all 100 uncertainty quantification calculations defined as the output parameter in Dakota coupled to the TRACE model of Test 012, compared to the nominal TRACE case without perturbed input parameters and the maximum and minimum range from the experiment [16].

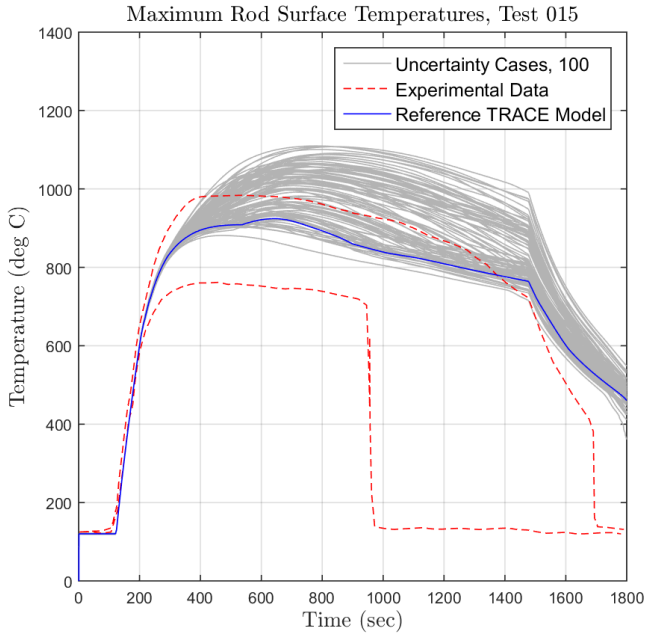

Figure 18. Peak cladding temperatures for all 100 uncertainty quantification calculations defined as the output parameter in Dakota coupled to the TRACE model of Test 015, compared to the nominal TRACE case without perturbed input parameters and the maximum and minimum range from the experiment [17].

5. DISCUSSION

The TRACE model results for both test cases of the SVEA spray cooling experiment indicate that there are sensitivities to specific parameters in the model that impact the peak cladding temperature prediction. From the Dakota random sampling of 100 cases of the TRACE model for Test 012 and Test 015, the 31 input parameters were compared in a sensitivity study. The Spearman rank correlation was chosen to examine non-parametric monotonic correlation between the input parameters to the peak cladding temperature, on the basis that many of the chosen parameters do not necessarily exhibit a linear relationship to PCT. Particularly, the CCFL model slope and constant values and many physical model sensitivity coefficients (which are factors of the TRACE-selected coefficient values and not the actual models' values) may not be accurately considered in a Pearson correlation. Therefore in a Spearman ranking, all of the parameter values are replaced with rank indices and then correlated using Equation 4. From the 100 cases, all 31 parameters are evaluated by their Spearman rank correlation to the output parameter (PCT), as well as their correlation to each other (Table 7, Table 8). The results indicate that there exists a strong correlation between several input parameters to the output parameter (PCT), but overall there is very little correlation between any two input parameters. This is the expected result, as Dakota uses Monte Carlo-based sampling on all of the input parameter distributions, so there should not be any significant correlation between the input parameters. If that were the case, then spurious correlations may falsify the significance of the erroneously-correlated input parameters to the results of the output parameter. It should be noted that the correlation values between each input parameter to the output parameter in the last rows of Table 7 and Table 8 also include the effects of all the other input parameters by nature (they do not describe the partial correlation).

Table 7. Spearman rank correlation coefficients across all 31 input parameters and the output parameter (peak cladding temperature) for 100 randomly sampled cases of the TRACE model for Test 012.

TEST 012 -- SPEARMAN RANK CORRELATION, 100 TESTS

	Bundle roughness	Bypass roughness	Water-cross roughness	Spray pressure	Spray temperature	Bundle spray flow	Bypass spray flow	Water cross spray flow	Water drain temp	Steam vent temp	Outlet pressure	Bundle length	Bypass length	Water-cross length	Bundle flow area	Bundle hydraulic dia.	Bypass flow area	Bypass hydraulic dia.	Water-cross flow area	Water-cross hydraulic dia.	Rod emissivity	Wall emissivity	CCFL slope	CCFL constant	DFFB Wall-Liq. HTC	Wall Liquid HTC	Wall Vapor HTC	Ann.-Mist Intf. Drag	DFFB Intf. Drag	Wall Drag	DNB/CHF	Peak Cladding Temperature
Bundle roughness	1.0																															
Bypass roughness	0.0	1.0																														
Water-cross roughness	0.0	0.0	1.0																													
Spray pressure	0.0	0.0	0.0	1.0																												
Spray temperature	0.0	0.0	0.0	0.0	1.0																											
Bundle spray flow	0.0	0.0	0.0	0.0	0.0	1.0																										
Bypass spray flow	0.0	0.0	0.0	0.0	0.0	0.0	1.0																									
Water cross spray flow	0.0	0.0	0.0	0.0	0.0	0.0	-0.1	1.0																								
Water drain temp	0.0	0.0	-0.1	0.0	0.0	0.0	0.0	0.0	1.0																							
Steam vent temp	0.0	0.0	0.0	0.0	0.0	0.0	0.0	0.0	0.0	1.0																						
Outlet pressure	0.0	0.0	0.0	-0.1	0.1	0.0	0.0	0.1	0.0	0.0	1.0																					
Bundle length	0.0	0.0	0.0	0.0	0.0	0.0	0.0	0.0	0.0	0.0	0.0	1.0																				
Bypass length	0.0	0.0	0.0	0.0	0.0	0.0	0.0	-0.1	0.0	0.0	0.1	0.0	1.0																			
Water-cross length	0.0	0.0	0.0	0.0	-0.1	0.0	0.0	0.0	-0.1	0.0	0.0	0.0	0.0	1.0																		
Bundle flow area	0.0	0.0	0.0	0.0	0.0	0.0	0.0	-0.1	0.0	0.0	-0.1	0.0	0.0	0.0	1.0																	
Bundle hydraulic dia.	0.0	0.0	0.0	0.0	0.0	0.0	0.0	0.0	0.0	0.1	0.0	0.0	0.0	0.0	0.0	1.0																
Bypass flow area	0.0	0.0	0.0	0.0	0.0	0.0	0.0	0.0	0.0	0.0	0.0	0.0	0.0	0.0	0.0	0.0	1.0															
Bypass hydraulic dia.	0.0	0.0	0.0	0.0	0.0	0.0	0.0	0.0	0.0	0.0	0.0	0.0	0.0	0.0	0.0	0.0	0.0	1.0														
Water-cross flow area	0.0	0.0	0.0	0.0	0.0	0.0	-0.1	0.0	0.0	0.0	0.0	0.0	0.0	0.0	0.0	0.0	0.0	0.0	1.0													
Water-cross hydraulic dia.	0.0	-0.1	0.0	-0.1	0.0	0.1	0.0	0.0	0.0	0.0	0.0	0.0	0.1	0.0	0.0	0.0	0.1	0.0	0.0	1.0												
Rod emissivity	0.0	0.0	0.0	0.0	0.0	0.0	0.0	0.0	0.0	0.0	0.0	0.0	0.0	0.0	0.0	0.0	0.0	0.0	0.0	0.0	1.0											
Wall emissivity	0.0	0.0	0.1	0.0	0.0	0.1	0.0	0.0	0.0	0.0	0.0	0.0	0.0	0.0	-0.1	0.0	0.0	0.0	0.0	0.1	0.0	1.0										
CCFL slope	0.0	0.0	0.0	0.0	0.0	0.0	0.0	0.0	0.0	0.0	0.0	0.0	0.0	0.0	0.0	0.0	0.0	0.0	0.0	0.0	0.0	0.0	1.0									
CCFL constant	0.0	0.0	0.0	0.0	0.0	0.0	0.0	0.0	0.0	0.0	0.0	0.0	0.0	0.0	0.0	0.0	0.0	0.0	0.0	0.0	0.0	0.0	0.0	1.0								
DFFB Wall-Liq. HTC	0.0	0.0	0.0	0.0	0.0	0.0	-0.1	0.1	0.0	0.0	0.0	0.0	0.0	0.0	0.0	0.0	0.0	0.0	0.0	0.0	0.0	0.0	0.0	0.0	1.0							
Wall Liquid HTC	0.0	0.0	0.0	0.0	0.0	0.0	0.0	0.0	0.0	0.0	0.0	0.0	0.0	0.0	0.0	0.1	0.0	-0.1	0.0	0.0	0.0	0.0	0.0	0.0	0.0	1.0						
Wall Vapor HTC	0.0	0.0	0.0	0.0	0.0	0.0	0.0	0.0	0.0	0.0	0.0	0.1	0.0	0.0	0.0	0.0	0.0	0.0	0.0	0.0	0.0	0.0	0.0	0.0	0.0	0.0	1.0					
Ann.-Mist Intf. Drag	0.0	0.0	0.0	0.0	0.0	0.0	0.0	0.0	0.0	0.0	0.0	0.0	0.0	0.0	0.0	0.0	-0.1	0.0	0.0	0.0	0.0	0.0	0.0	0.0	0.0	0.0	0.0	1.0				
DFFB Intf. Drag	0.0	0.0	0.0	0.0	0.0	0.0	0.0	0.0	0.0	0.0	0.1	0.0	0.0	0.0	0.0	0.0	0.0	0.0	0.0	0.0	0.0	0.0	0.0	0.0	0.0	0.0	0.0	0.0	1.0			
Wall Drag	0.0	0.0	0.0	0.0	0.0	0.0	0.0	0.0	0.0	0.0	0.0	0.0	0.0	0.0	0.0	0.0	0.0	0.0	0.0	0.0	0.0	0.0	0.0	0.0	0.0	0.0	0.0	0.0	0.0	1.0		
DNB/CHF	0.0	0.0	0.0	0.0	-0.1	0.0	0.0	0.0	0.0	0.0	0.0	0.0	0.0	0.0	0.0	0.0	0.0	0.0	0.0	0.0	0.0	0.0	0.0	0.0	0.0	0.0	0.0	0.0	0.0	0.0	1.0	
Peak Cladding Temperature	0.0	0.0	0.0	0.0	0.0	0.0	0.0	0.0	0.0	0.0	-0.1	0.1	0.0	-0.1	-0.1	0.0	0.1	0.0	-0.1	0.0	-0.3	-0.1	0.3	-0.8	0.2	0.0	0.1	0.0	0.0	0.0	0.0	1.0

Color-coding scheme	
0.5	Max Value
-0.5	Min Value

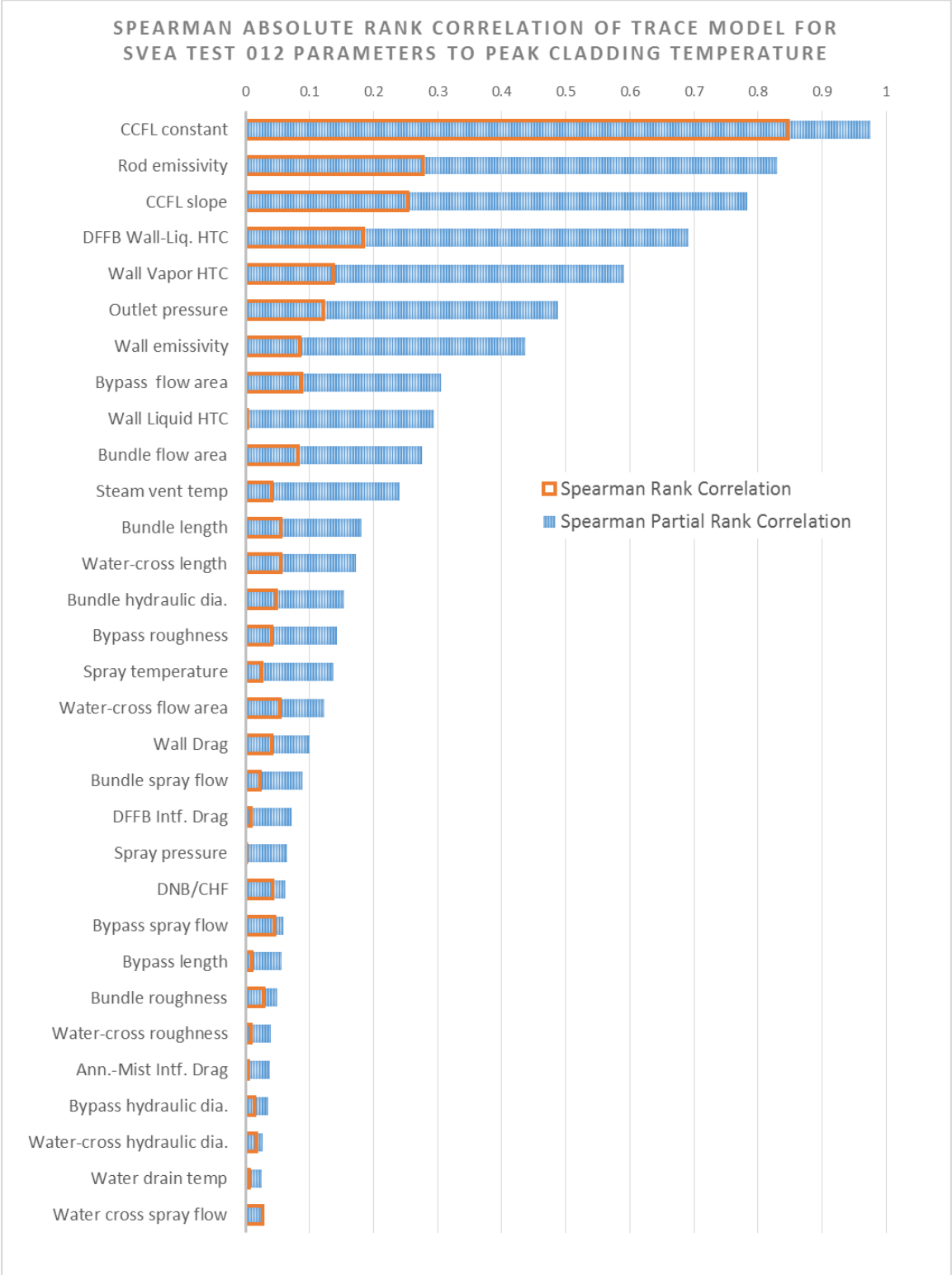

Figure 19. Spearman absolute rank correlation over all 31 input parameters of the TRACE model for Test 012 compared to the output parameter (PCT). Both the regular Spearman coefficient and the Spearman partial correlation coefficient are plotted.

Table 8. Spearman rank correlation coefficients across all 31 input parameters and the output parameter (peak cladding temperature) for 100 randomly sampled cases of the TRACE model for Test 015

TEST 015 -- SPEARMAN RANK CORRELATION, 100 TESTS

	Bundle roughness	Bypass roughness	Water-cross roughness	Spray pressure	Spray temperature	Bundle 1 spray flow	Bundle 2/3 spray flow	Bundle 4 spray flow	Bypass spray flow	Water cross spray flow	Water drain temp	Steam vent temp	Outlet pressure	Bundle length	Bypass length	Water-cross length	Bundle flow area	Bundle hydraulic dia.	Bypass flow area	Bypass hydraulic dia.	Water-cross flow area	Water-cross hydraulic dia.	Rod emissivity	Wall emissivity	CCFL slope	CCFL constant	DFFB Wall-Liq. HTC	Wall Liquid HTC	Wall Vapor HTC	Ann.-Mist Intf. Drag	DFFB Intf. Drag	Wall Drag	DNB/CHF	Peak Cladding Temperature
Bundle roughness	1.0																																	
Bypass roughness	0.0	1.0																																
Water-cross roughness	-0.1	0.0	1.0																															
Spray pressure	0.0	0.0	0.0	1.0																														
Spray temperature	0.0	0.0	0.0	0.0	1.0																													
Bundle 1 spray flow	0.0	0.0	0.0	0.0	0.0	1.0																												
Bundle 2/3 spray flow	0.0	0.0	0.0	0.0	0.0	0.0	1.0																											
Bundle 4 spray flow	0.1	0.0	0.0	0.0	0.0	0.0	0.0	1.0																										
Bypass spray flow	0.0	0.0	0.0	0.0	0.0	0.0	0.0	0.0	1.0																									
Water cross spray flow	0.0	0.0	0.0	0.0	0.0	0.0	0.0	0.0	0.0	1.0																								
Water drain temp	0.1	0.0	0.0	0.0	0.0	0.0	0.0	0.0	0.0	0.0	1.0																							
Steam vent temp	0.0	0.0	0.0	0.0	0.0	0.0	0.0	0.0	0.0	0.0	0.0	1.0																						
Outlet pressure	0.0	0.0	0.0	0.0	0.0	0.0	0.0	0.0	0.0	0.0	0.0	0.0	1.0																					
Bundle length	0.0	0.0	0.0	0.0	0.0	0.0	0.0	0.0	0.0	0.0	0.0	0.0	0.0	1.0																				
Bypass length	0.0	0.0	0.0	0.0	0.0	0.0	0.0	0.0	0.0	0.0	0.0	0.0	0.0	0.0	1.0																			
Water-cross length	0.0	0.0	0.0	0.0	0.0	0.0	0.0	0.0	0.0	0.0	0.0	0.0	0.0	0.0	0.0	1.0																		
Bundle flow area	-0.1	0.0	0.0	0.0	0.0	0.0	0.0	0.0	0.0	0.0	0.0	0.0	0.0	0.0	0.0	0.0	1.0																	
Bundle hydraulic dia.	-0.1	0.0	0.0	0.0	0.0	0.0	0.0	0.0	0.0	0.0	0.0	0.0	0.0	0.0	0.0	0.0	0.0	1.0																
Bypass flow area	0.0	0.0	0.0	0.0	0.0	0.0	0.0	0.0	0.0	0.0	0.0	0.0	0.0	0.0	0.0	0.0	-0.1	0.0	1.0															
Bypass hydraulic dia.	0.0	0.0	0.0	0.0	-0.1	0.0	0.0	0.0	0.0	0.0	0.0	0.0	0.0	0.0	0.0	0.0	0.0	0.0	0.0	1.0														
Water-cross flow area	0.0	0.0	0.0	0.0	0.0	0.0	0.0	-0.1	0.0	0.0	0.0	0.0	0.0	0.0	0.0	0.0	0.0	0.0	0.0	0.0	1.0													
Water-cross hydraulic dia.	0.0	0.0	0.0	0.0	0.0	0.0	0.0	0.0	0.0	0.0	0.0	0.0	0.0	0.0	0.0	0.0	0.0	0.0	0.0	0.0	0.0	1.0												
Rod emissivity	0.0	0.0	0.0	0.0	0.0	0.0	0.0	0.0	0.0	0.0	0.0	0.0	0.0	0.0	0.0	0.0	0.0	0.0	0.0	0.0	0.0	0.0	1.0											
Wall emissivity	0.0	0.0	0.0	0.0	0.0	0.0	0.0	0.0	0.0	0.0	0.0	0.0	0.0	0.0	0.0	-0.1	0.0	0.0	0.0	0.0	0.0	-0.1	0.0	1.0										
CCFL slope	0.0	0.0	0.0	0.0	0.0	0.0	-0.1	-0.1	0.0	0.0	0.0	0.0	0.0	0.0	0.0	0.1	0.0	0.0	0.1	0.0	0.0	0.1	0.0	0.0	1.0									
CCFL constant	0.1	0.0	0.0	0.0	0.0	0.0	0.1	0.0	0.0	0.1	0.0	0.0	0.0	0.0	0.0	0.0	0.0	0.0	0.1	0.0	0.0	0.0	0.0	0.0	0.0	1.0								
DFFB Wall-Liq. HTC	0.0	0.0	0.0	0.0	0.0	0.0	0.0	0.0	0.0	0.0	0.0	0.0	0.0	0.0	0.0	0.0	0.0	0.0	0.0	0.0	0.0	0.0	0.0	0.0	0.0	0.0	1.0							
Wall Liquid HTC	0.0	0.0	0.0	0.0	0.0	0.0	0.0	0.0	0.0	0.0	0.0	0.1	0.0	0.0	0.0	0.0	0.0	0.0	0.0	0.0	0.0	0.0	0.0	0.0	0.1	0.0	0.0	1.0						
Wall Vapor HTC	0.0	0.0	0.0	0.0	0.0	0.0	0.0	0.0	0.0	0.0	0.0	0.0	0.0	0.0	0.0	0.0	0.0	0.0	0.0	0.0	0.0	0.0	0.0	0.1	0.0	0.0	0.0	0.0	1.0					
Ann.-Mist Intf. Drag	0.0	0.0	0.0	0.0	0.0	0.0	0.0	0.0	0.0	0.0	0.0	0.0	0.0	0.0	0.0	0.0	0.0	0.1	0.0	0.0	0.0	0.0	0.0	0.0	0.0	0.0	0.0	0.0	0.1	1.0				
DFFB Intf. Drag	0.0	-0.1	0.1	0.0	0.0	0.0	0.0	0.0	0.0	0.0	0.0	0.0	0.0	0.0	0.0	0.0	0.0	0.0	0.0	0.0	0.0	0.0	0.0	0.0	0.1	0.0	0.0	0.0	0.0	0.0	1.0			
Wall Drag	0.0	0.0	0.1	0.0	0.0	0.0	0.0	0.0	0.0	0.0	0.0	0.0	0.0	0.0	0.0	0.0	0.0	0.1	0.0	0.0	0.0	0.0	0.0	0.0	0.0	-0.1	0.0	0.0	0.0	0.0	0.0	1.0		
DNB/CHF	0.0	0.0	0.0	0.0	0.0	0.0	0.0	0.0	0.0	0.0	0.0	0.0	0.0	0.0	0.0	0.0	0.0	0.0	0.0	0.0	0.0	0.0	0.0	0.0	0.1	0.0	0.0	0.0	0.0	0.0	0.0	0.0	1.0	
Peak Cladding Temperature	0.0	0.0	0.0	0.0	0.0	0.0	-0.1	-0.1	0.0	-0.1	0.0	0.0	-0.1	0.0	0.0	0.0	-0.1	0.0	-0.1	0.0	0.0	0.0	-0.2	-0.2	0.2	-0.9	0.2	0.0	0.1	0.0	0.0	0.1	0.0	1.0

Color-coding scheme	
0.5	Max Value
-0.5	Min Value

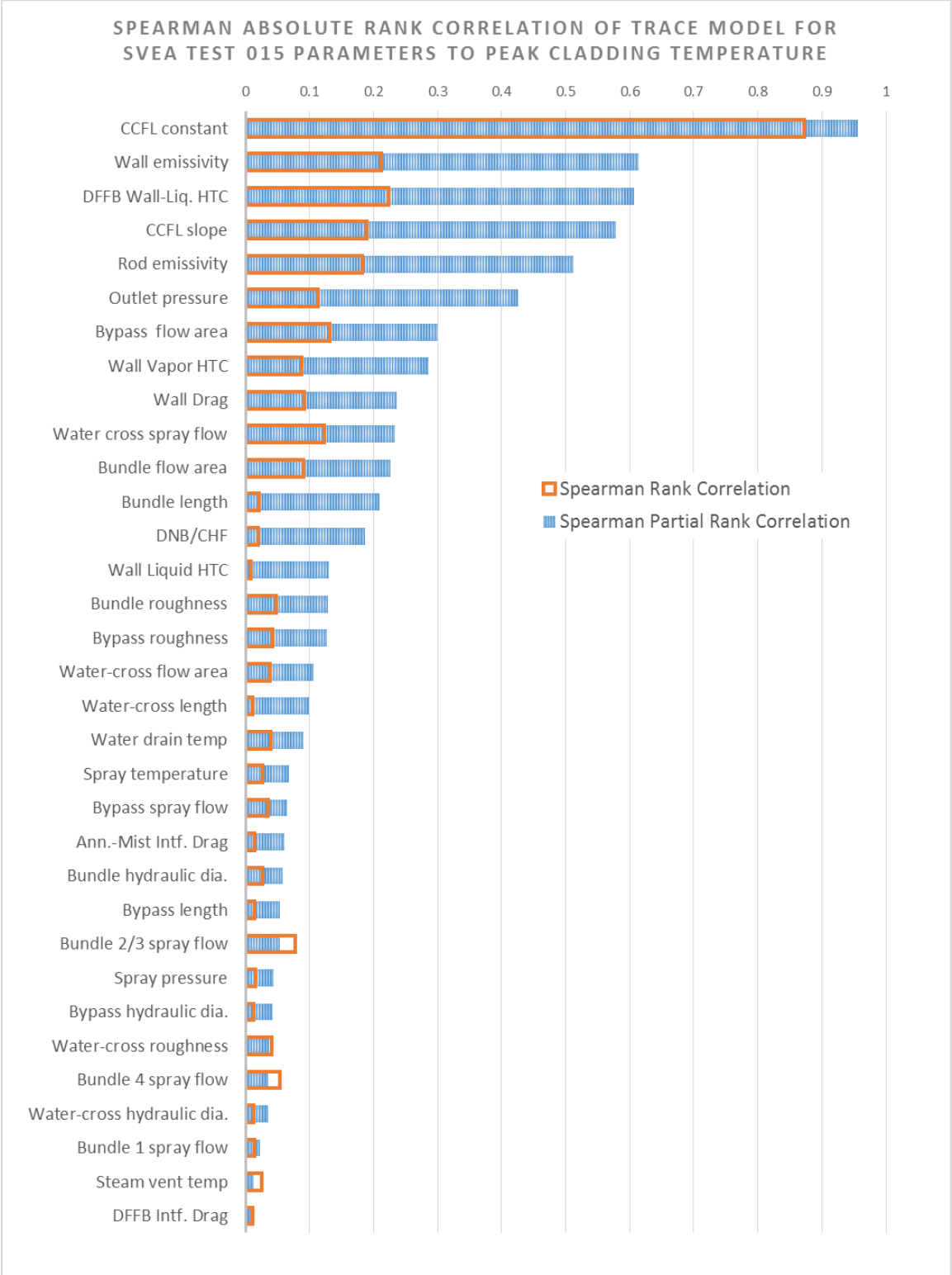

Figure 20. Spearman absolute rank correlation over all 31 input parameters of the TRACE model for Test 015 compared to the output parameter (PCT). Both the regular Spearman coefficient and the Spearman partial correlation coefficient are plotted.

The partial correlation of the Spearman rank correlations for the 31 input parameters to the output parameter (PCT) is also evaluated in Dakota, and the input parameters were ordered by their partial correlation rank value to determine the most sensitive parameters (Figure 19, Figure 20). The two most significant parameters are the CCFL constant and the rod/wall surface emissivity, which are both TRACE model parameters. The result indicates that the CCFL phenomenon has a significant effect on prediction of PCT in reflood scenarios under spray cooling, and an accurate understanding of this phenomenon and how to model its effects should be the primary focus [9]. CCFL mitigating fluid flow into the fuel rod region also leads to greater significance in accurately determining the radiation heat transfer, which is demonstrated by the high ranking of the rod and wall emissivity parameters in the uncertainty analysis. In Test 015, it is postulated that wall emissivity plays a larger role compared to Test 012 due uneven spray distribution resulting in heat transfer from the starved sub-bundle to the surrounding cooler sub-bundles through radiation heat transfer to the water-cross channel. The base TRACE model was re-evaluated with a modified CCFL model to determine the most conservative prediction (with a model slope value of 1.0 and constant value of 0.88) to examine the findings from the uncertainty analysis (Figure 21). In agreement with the uncertainty analysis, the modification of the CCFL model was found to have a significant effect at the axial middle of the bundle (level 3), where the cladding temperatures were predicted higher near the maximum of the range of the experimental measurements. At the bottom of the bundle (level 1), the CCFL model modifications had little effect, but at the top of the bundle (level 5), the modifications resulted in significantly delayed quenching with similar PCT prediction. This latter result indicates that TRACE predicts the CCFL phenomenon does mitigate spray coolant flow entering the top of the core.

Test 012 – Uniform Spray Flow Conditions, Modified CCFL Model Comparison

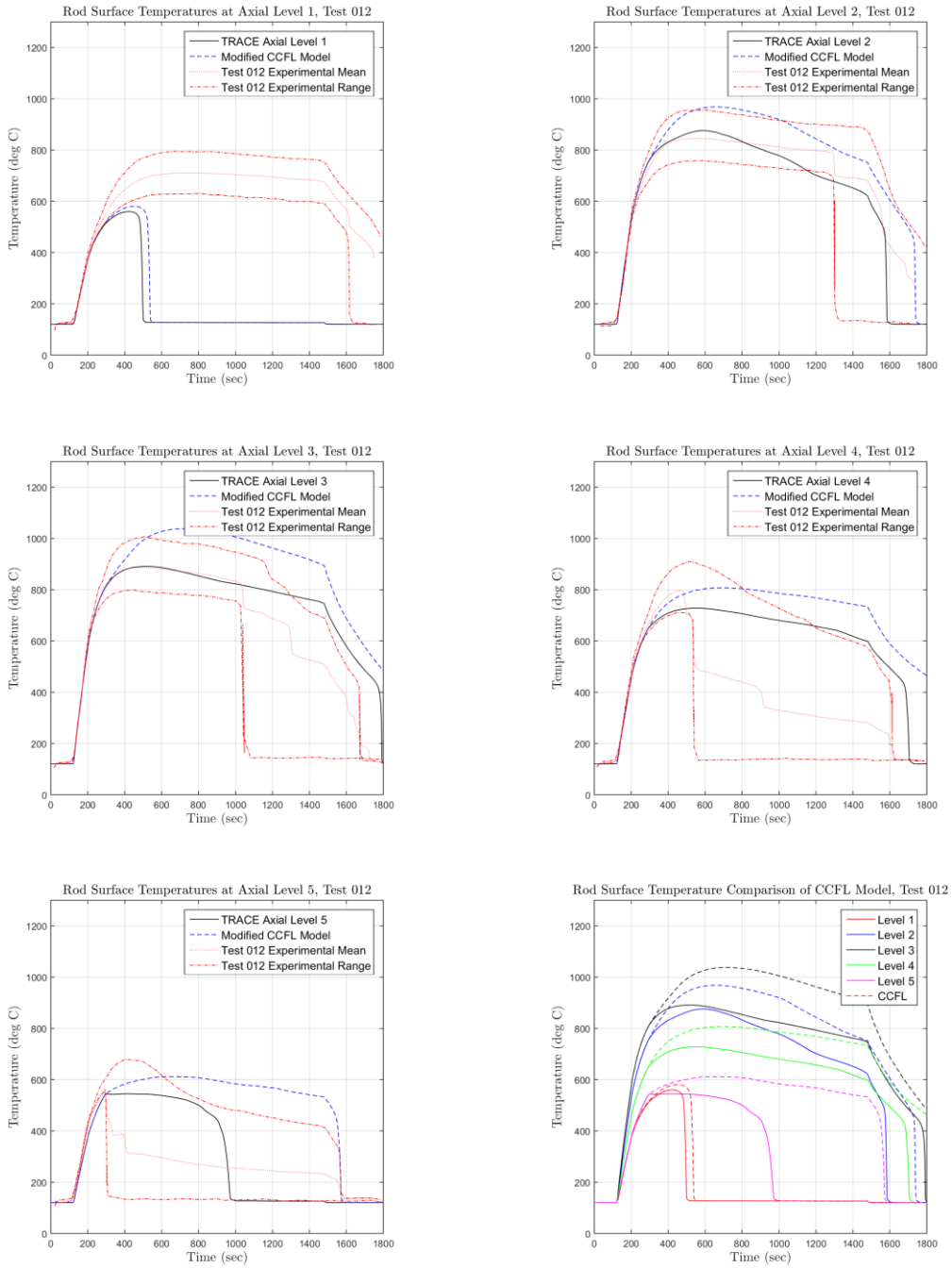

Figure 21. Comparison of TRACE peak cladding temperature prediction with modifications to the CCFL model based on the performed uncertainty analysis. Experimental data is also plotted. Comparisons are made at 5 axial locations, from the bottom of the bundle at level 1 (top left) up to the top of the bundle at level 5 (bottom left). All axial TRACE predictions are compared together (bottom right).

The highest-ranked sensitivity coefficient parameters (physical model coefficients selected by TRACE during the simulation) are the heat transfer coefficients for dispersed flow film boiling (DFFB) wall-liquid (rod surface to spray droplets) and single-phase wall-vapor (steam convection). This sensitivity is expected, since the dominating fluid flow regime during the occurrence of PCT is dispersed film flow boiling. This is predicted by the Yamanouchi model [6] in Phase II cooling, where droplets may exist in the bulk region between fuel rods, but the cladding surface has not been quenched yet by the falling film (Figure 1). However, it is difficult to justify any significance in comparing the input parameters beyond the seven highest ranked parameters, as their partial rank correlation values fall below 0.3. This is evident in the comparison between the two uncertainty quantification analyses performed for Test 012 and Test 015, for which the highest ranked parameters are relatively consistent, but the remaining parameters have low partial rank correlation values. Furthermore, this observation was confirmed by plotting the sampled input parameter values from Test 012 against the peak cladding temperature for all 100 uncertainty cases (Figure 22). The TRACE model demonstrates a strong correlation for the CCFL constant, and a discernible trend for the rod emissivity. However, determining such a correlation by visual means is not possible for even the highly-ranked DFFB wall-liquid and single-phase wall-vapor heat transfer coefficients (although a correlation can still be fit to the data by numerical analysis). Therefore, out of the 31 parameters considered, about 5-7 have a significant influence on the prediction of PCT whereas the remaining parameters do not exhibit significant sensitivity in the performance of the TRACE model.

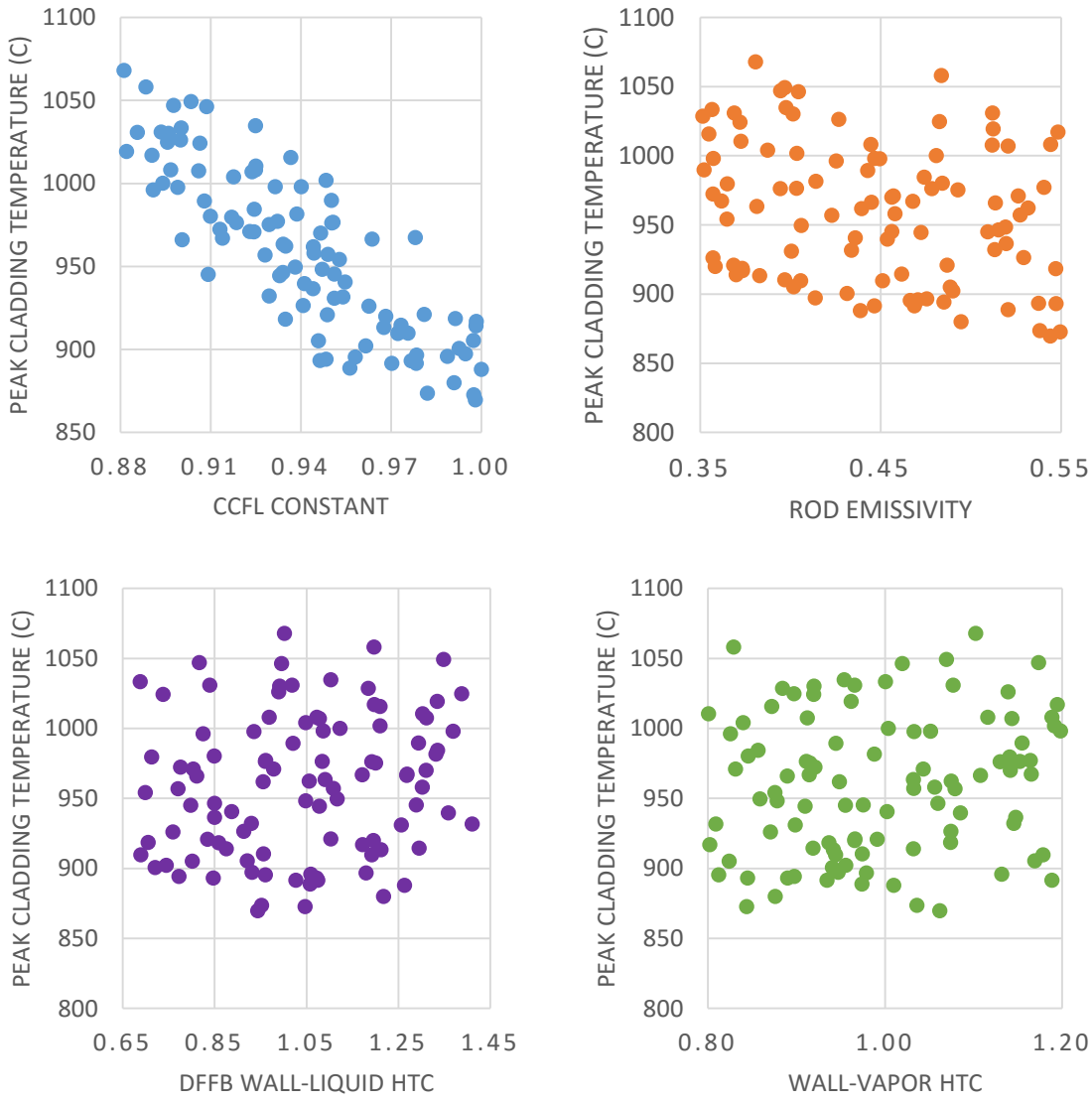

Figure 22. Comparison of the highest-ranked input parameter values to the output parameter (PCT) of the uncertainty quantification of the TRACE model for Test 012.

6. CONCLUSION

In this work, the physical phenomena involved in the emergency spray cooling injection in a Swedish-designed reactor with SVEA-type fuel assemblies was examined. The US NRC thermal-hydraulic code TRACE version 5.0 Patch 4 was used to develop a simulation model, and was coupled to Dakota to perform forward uncertainty quantification on 54 input parameters in the TRACE model input. The developed simulation model was able to provide a reasonable prediction of the trend of the transient peak cladding temperature, and the uncertainty analysis provided insight into various model parameters that have significant impact to reflood-type simulations. Overall the uncertainty analysis also indicated that over the range of uncertainties in the model input, TRACE is able to predict the range of cladding temperatures measured from the experiment.

From the uncertainty quantification analysis using Dakota, the most influential parameters were related to the CCFL model and rod/wall emissivity. These parameters are related to physical phenomena (CCFL and radiation heat transfer) that are expected to occur in the initial stages of reflood prior to the incipience of PCT, largely governing the amount to which the fuel rod will heat up due to decay heat before mitigation due to ECCS injection. This result emphasizes that an accurate understanding of CCFL effects during reflood and determination of the radiation model is essential for accurate simulation of emergency BWR spray cooling systems. From the physical model sensitivity coefficients, the TRACE model was particularly sensitive to the dispersed flow film boiling (DFFB) and single-phase wall-vapor (steam convection) coefficients, which correspond to the flow regime expected at the point that peak cladding temperature is reached in a BWR LOCA reflood scenario with spray cooling present. The overall results of this work demonstrate the capabilities of codes with the philosophy of best estimate plus uncertainty and particularly that TRACE can be used for validation of comprehensive experiments such as

spray cooling over SVEA fuel bundles. Additionally, this work indicates where uncertainties are acceptable in relation to this type of reflooding simulation, with the understanding that the sensitivity of those parameters to the overall model performance is minor or insignificant. All-in-all, this work demonstrates that BEPU-philosophy codes are very capable of accurate, reliable simulation that increase the assurance in determining nuclear reactor safety performance and prediction of reliability.

6.1 Future Work

The revelation of sensitivities to model parameters related to CCFL and rod/wall emissivity indicate that future work must be performed both in dedicated experimental study and in computational simulation effort to more accurately determine the causes and correlations of these reflood-related phenomena to the performance of nuclear reactor safety systems. There has been significant work in understanding CCFL effects and developing an accurate model in TRACE, but there are still limitations in using a 1-D simulated model to evaluate the effects of CCFL. Additionally, there are ongoing efforts to accurately develop a droplet model and establish a droplet field within the TRACE code [18] to vastly improve the simulation capability of reflood prediction, as the droplet model has significant impact modeling the constitutive terms in DFFB flow, as well as having a recognizable impact on the modeling of radiation heat transfer. A separate droplet field in TRACE would also allow consideration of spray flow distribution, which differs between varying types of BWR emergency cooling designs. A greater-detailed analysis of the radiation model capabilities of TRACE with regards to the present scenario would reveal valuable understanding of PCT prediction capability and would underscore the benefits and limitations of the SVEA-64 fuel bundle design. Developing a more accurate radiation model in TRACE may increase differentiation between the fuel rod temperatures and overall prediction of PCT with improved validation to the experimental data.

APPENDIX A. RADIATION HEAT TRANSFER MODEL

In the present work, the methodology implemented to model the average sub-bundle rod radiation heat transfer in the TRACE computational model is presented here. Additionally, an assessment of the radiative and convective heat transfer significance based on the experimental data is also conducted. This section demonstrates the conservatism and justification for the radiation heat transfer treatment in the experimental and computational work.

A.1 TRACE Average Radiation Model

The TRACE model implemented in this work uses one HTSTR heat-structure component within one PIPE hydraulic component to model 4 x 4 sub-bundle assembly in the SVEA test assembly. As a result, the heat transfer behavior of the component modeling the heater rods represents an averaged heater rod out of the 16 rods comprising the sub-bundle assembly. The geometric modeling of the heater rod and bundle hydraulic flow area is explicitly defined in the TRACE model input (in the HTSTR and PIPE component inputs, respectively), however the RAD radiation power component is unable to explicitly differentiate the view factors for all 16 rods, as only a single averaged rod is represented, and the interaction between individual heater rods is not considered in this TRACE model. Within a single sub-bundle, there are 3 radiation surfaces that are considered that area each represented by their own HTSTR heat structure components: the heater rod surface, the bypass wall surface, and the water cross wall surface. There are four individual sets of these radiation surfaces (one set for each sub-bundle), and each HTSTR component is coupled to its corresponding PIPE hydraulic component (bypass wall coupled to the bypass channel, etc.) to model the convective heat transfer to their respective hydraulic flow regions. The first radiation model defines the radiation heat

transfer between the three aforementioned radiation surfaces, for which appropriate view factors must be defined in the TRACE input model, along with the surface emissivities. The surface emissivity values were taken from the experiment documentation [2] and were evaluated in the uncertainty analysis portion of the present work. The view factors were also taken from documentation [2], and are given for rod-to-rod and rod-to-wall for the central, side (adjacent to wall), and corner rod groupings. In order to average the radiation heat transfer from rod-to-wall for the TRACE model, the mean of all 16 rod view factors was used to give the average rod-wall view factor in a sub-bundle.

Table 9. Rod-to-wall view factors for a single sub-bundle taken from SVEA experiment documentation [2], and the average of all 16 heater rod view factors used to model the averaged heater rod in TRACE.

Rod Location	No. of Rods	Wall View Factor
Central	4	0.0736
Side	8	0.447
Corner	4	0.4189
TRACE Average	1	0.3466

As there are two radiation wall surfaces defined in the TRACE model (for the bypass and water-cross), half of the average view factor was attributed to radiation from the heater rod to the bypass wall and half was attributed to radiation from the heater rod to the water cross wall since both wall surfaces are symmetric and relatively have the same surface area exposed to the heater rods. Thus the fraction of rod-to-wall radiation heat transfer surface area for the sub-bundle as a whole is preserved. It is noted that in this simplified TRACE model, the rod-to-rod radiation heat transfer is not modeled. As the PCT typically occurs at one of the central rods in the sub-bundle assembly, this lack of rod-to-rod radiation heat transfer may have resulted in some over-prediction of PCT since there is no radiation heat transfer modeled from the central heater rods to the cooler surrounding rods that are adjacent to a wall surface.

A.2 SVEA Experiment Convective and Radiation Heat Transfer Study

An assessment of the amount of heat transfer attributed to radiation was conducted for the experiment data from SVEA Test 012. The intention was to roughly determine the contribution of radiation heat transfer and convective heat transfer, to estimate the significance of the radiation model in TRACE. The heat transfer balance between the heater rod to the rest of the sub-bundle is defined by the heater rod power (q''_{total}) and the radiation ($q''_{radiation}$) and convective ($q''_{convection}$) heat transfer rates:

$$q''_{total} = q''_{convection} + q''_{radiation}$$

$$q''_{convection} = h_{rod}\left(T_{clad} - T_{bulk}\right)$$

$$\frac{q''_{radiation}}{q''_{total}} = 1 - \frac{q''_{convection}}{q''_{total}} \tag{5}$$

From this heat transfer balance, we can roughly determine the amount of convective heat transfer for a single heater rod, and estimate the ratio of convective to radiation heat transfer given the heater rod power and rod surface temperatures (T_{clad}) from Test 012 measurements [16]. This assessment was made for the three rod groupings defined previously for the radiation model (central, side, and corner) and their convective heat transfer coefficients (h_{rod}) were taken from the experiment documentation [2]. The convective heat transfer was assessed at 300 seconds and at 1000 seconds to determine the heat transfer mechanism before and after PCT is reached, but before quenching is observed to occur at the axial mid-plane (axial level 3). The bulk fluid (T_{bulk}) is assumed to be at saturation at the Test 012 vessel pressure of 2 bar, and the total heater rod surface area is determined from the geometries and active heater length from the experiment documentation to obtain the total heat flux for a single heater rod. The test bundle power distribution between heater rods was measured to be nominally equal [2], so the same total heat flux has been assumed for all three rod location groups.

Table 10. Assessment of convection and radiation heat transfer at different rod locations in a SVEA-64 sub-bundle assembly. Convective heat transfer coefficients were taken from documentation [2], and bundle power and cladding temperatures were taken from Test 012 [16].

Rod Location		Central	Side	Corner
HTC (W/m2-°C) [2]		10.6	17.3	15.0
Before PCT (300 sec)	Bundle Power (KW)	225	225	225
	Cladding Temperature (°C)	900	800	775
	Convection-to-Total Heat Flux Ratio	0.33	0.47	0.40
	Radiation-to-Total Heat Flux Ratio	0.67	0.53	0.60
After PCT (1000 sec)	Bundle Power (KW)	160	160	160
	Cladding Temperature (°C)	975	800	750
	Convection-to-Total Heat Transfer Ratio	0.51	0.67	0.54
	Radiation-to-Total Heat Flux Ratio	0.49	0.33	0.46

From the assessment performed, it is evident that radiation heat transfer is dominant prior to the point of PCT, but is not dominant after PCT has occurred. The higher convective heat transfer coefficients at the side and corner rod locations are most likely due to the effects of the spray flow distribution, where a majority of the upward steam flow will occur in the central region of the bundle, with falling liquid moving towards the outer region of the bundle and collecting on the cooler wall surfaces in the sub-bundle channel. This phenomena is even more relevant following the point of PCT, where convection heat transfer will dominate as continuous spray flow leads to falling liquid reaching further down the channel. The radiation-to-total heat flux ratio is highest for the central rods prior to PCT, which indicates that radiation heat transfer is a very significant heat transfer mechanism that will govern the point of the peak cladding temperature.

Chiou and Hochreiter [32] also performed a best-estimate simulation of the SVEA spray cooling experiments using COBRA-TF (WCOBRA/TRAC) shortly after the tests were concluded. Their study included a detailed analysis of the radiation heat transfer in

the SVEA-64 fuel bundle under spray cooling, with several assessments of the phenomena that were observed to occur during the experiment contributing to PCT.

The detailed radiation model determined the rod emissivity to be 0.6 and the wall surface emissivity to be 0.96 with the assumption that the bypass and water-cross walls were wetted during the experiment. The study concluded that the experimental flow regime in the test bundle was highly dispersed concurrent and countercurrent two-phase flow (DFFB), with the void fraction near unity. The radiation heat transfer dominated (greater than 90%) primarily by rod-to-rod and rod-to-surface radiation heat transfer. Additionally, the study for an extreme non-uniform spray flow case (with one sub-bundle receiving no spray flow) indicated that PCT rise was still mitigated even in the extreme case due to the effective transfer of heat by radiation to the water-cross and to the surrounding sub-bundles. This observation was also found in the present TRACE predictions that show similar cladding temperatures across all four sub-bundles in the Test 015 non-uniform spray flow case.

APPENDIX B. UNCERTAINTY INPUT PARAMETER SELECTION METHODOLOGY

The consideration and selection of a model's input parameter uncertainties have a significant impact on the resulting uncertainty and sensitivity assessment that can be performed. It is necessary to have some level of comprehension with regard to the input parameters and their probable impact on the physics rendered in a computational model, as well as to have a realistic scope of a parameter's uncertainty when performing sensitivity comparisons between input parameters. The following sections describe the methodology implemented in selection of the uncertainty input parameters in this work, along with some justification for the assessment of the input parameter uncertainties.

B.1 Experiment Modeling Parameters

For the developed TRACE model simulating the SVEA spray cooling test facility, several parameters related to the determination of parameters related to modeling the test bundle components were assessed for their sensitivity to the peak cladding temperature. Parameters 1-8 assess the sensitivity of the experiment test conditions and measurement accuracy, particularly for thermal-hydraulic boundary conditions such as pressure, flow rate, and temperature for spray inlets, drain outlets and steam vent outlets. The uncertainties in these parameters were taken directly from the experiment documentation [2]. Parameters 9-14 assess the sensitivity of dimensional parameters for the test vessel, particularly for wall roughness and axial length of components. The uncertainty for wall roughness (parameters 9-11) was determined from recommendations by Wickett, D'Auria and Glaeser [21] as a reasonable range in best-estimate thermal hydraulic code modeling. The uncertainty in the length of the test vessel channels (parameters 12-14) was assessed by considering variability in machining of these components and in the deformation and expansion that could possibly occur during experiment. Linear thermal expansion of

Zircaloy-4 alloy (the material used in the construction of the test vessel components) over the range of temperatures in the experiment could lead to axial length uncertainty on the order of several millimeters. For this study, 1.0 cm was taken as a conservative estimate of the axial length uncertainty, as it is assumed that structural integrity of the test bundle would limit this amount of thermal expansion. Furthermore, manufacturing tolerances for a machined metallic component on the order of a few meters in length would not be expected to be larger than this uncertainty. Parameters 15-24 assess the parameters involved in modeling the test bundle itself, along with the considered phenomenological models implemented in TRACE for CCFL and for radiation heat transfer. For flow area and hydraulic diameter (parameters 15-19), the uncertainties in these values have been taken from expert recommendation from D'Auria, Bousbia-Salah, and Petruzzi [22] as well as recommendations from previous benchmark exercise performed for the NUPEC BWR Full-size Fine-mesh Bundle Tests [25]. For both flow area and hydraulic diameter, both are recommended to assess the uncertainty of these parameters conservatively to 1% as error due to manufacturing tolerances or from any geometric distortion due to forces in the experiment. The uncertainties in the surface emissivity values (parameters 21-22) for the radiation heat transfer model was taken from the original documentation describing a radiation heat transfer assessment performed for the SVEA spray cooling test bundle. For the CCFL model, the range of values for the Wallis-model CCFL slope m and constant C were taken from his own original work that established model for annular-mist flow [24].

B.2 TRACE Physical Model Parameters

The physics portrayed in TRACE is simulated by a two-fluid model for two-phase flow, for which a number of constitutive and closure models must be used for completeness. These physical models govern the conservation of mass, momentum and energy exchange between the fluid phases and vary according to the type of two-phase flow regime. In TRACE, 38 parameters related to these physical models are presented as user-

input sensitivity coefficient options to assess their impact on TRACE simulation capability [33]. An initial selection out of these 38 parameters was made to exclude several parameters that do not relate to the present model (parameters related to nuclear fuel rods, horizontal flows, specific TRACE components not implemented, etc.). The initial list of 26 physical model parameters (Table 11) defined the heat transfer coefficients and interfacial drag coefficients used by TRACE for different flow regimes.

Table 11. Initial list of 26 considered TRACE physical model sensitivity coefficients. The bolded parameters were observed to be sensitive to the prediction of PCT in the present TRACE model in a scoping study.

Heat Transfer Coefficients	Interfacial Drag Coefficients
Bubbly-Slug Liquid-Interface HTC	Bubbly Interfacial Drag
Bubbly-Slug Vapor-Interface HTC	Churn Interfacial Drag
Annular-Mist Liquid-Interface HTC	Annular Interfacial Drag
Annular-Mist Vapor-Interface HTC	Bubbly-Slug Interfacial Drag
Transition Liquid-Interface HTC	**Annular-Mist Interfacial Drag**
Transition Vapor-Interface HTC	**DFFB Interfacial Drag**
DFFB Wall-Liquid HTC	Droplet Interfacial Drag
Wall Liquid HTC	Inverted Slug Interfacial Drag
Wall Vapor HTC	Inverted Annular Interfacial Drag
Inverted Annular Wall-Liquid HTC	**Wall Drag**
Inverted Annular Wall-Vapor HTC	**Physical Model Coefficients**
Subcooled Boiling HTC	**DNB/CHF**
Nucleate Boiling HTC	Flooding Temperature Coefficient
Transition Boiling HTC	Flood Length Coefficient

A preliminary scoping study was performed to determine which of the 26 parameters exhibited sensitivity to the modeling of PCT in the present TRACE model by performing 26 individual TRACE simulations with a single sensitivity coefficient set to 500% of its original value. Only 7 parameters were observed to have a significant impact on the prediction of PCT, with a large portion of the parameters having no effect whatsoever. A few parameters exhibited some effect on the predicted cladding temperature at axial levels corresponding to the top or bottom of the fuel bundle, but did not impact the overall prediction of PCT which occurs at the axial mid-plane. The present uncertainty analysis work uses a single bundle-inclusive PCT value as the output parameter, so these few

parameters would not demonstrate correlation in the overall uncertainty analysis and were not included in the considered set. The remaining 7 parameters exhibiting sensitivity to PCT prediction correspond to flow regimes that are expected in post-CHF conditions, which largely determine the heat transfer governing in the initial stages of spray cooling that lead up to the incidence of PCT in a LOCA scenario.

Parameters 25-28 (Table 5) assess the heat transfer coefficients primarily for wall-to-fluid in post-CHF flow regimes. The scoping study revealed that interfacial heat transfer was not observed to play a large role in predicting PCT, as the majority of convective heat transfer would more likely exist between the wall and fluid rather than between the two fluid phases. For these heat transfer coefficients, the TRACE theory manual [18] was consulted to determine the correlations used in the code, and the uncertainties were found from their original literature or TRACE assessment studies. Parameters 29-31 assess the interfacial drag coefficients that determine the momentum transfer between the two phases. Particularly important in the case of spray cooling is the interfacial drag of the discontinuous liquid phase in vapor up-flow (spray droplets) as well as the interfacial drag on the annular liquid film that progresses downward with quenching. For TRACE, these are modeled by the Annular-Mist and Dispersed Flow Film Boiling (DFFB) interfacial drag coefficients (parameters 29 and 30). The Wallis model is used in TRACE to model rough annular film interfacial drag, and the uncertainty was taken from the original literature [24]. No specific literature was found to specifically address the uncertainty of DFFB interfacial drag, but the uncertainty of the droplet entrainment rate was quantified by Ishii and Kataoka [29]. As the entrainment rate plays a large factor in determining DFFB interfacial drag in the methodology used by TRACE, the uncertainty in the entrainment rate at 40% was adopted for DFFB interfacial drag. The uncertainty for wall drag (parameter 31) was taken from work by Zigrang and Sylvester [30] assessing the prediction of Colebrook's friction factor used to determine wall drag in TRACE.

REFERENCES

[1] F. D'Auriaa and O. Mazzantini, "The Best-Estimate Plus Uncertainty (BEPU) Challenge in the Licensing of Current Generation of Reactors," in *International Conference on Opportunities and Challenges for Water Cooled Reactors in the 21. Century*, Vienna, Austria, 2009.

[2] R. Eklund, M. O. Bäckwall and H. Wijkström, "SVEA Spray Cooing Test: Test Results and Evaluation," ASEA-ATOM, 1987.

[3] OECD Nuclear Energy Agency, "Nuclear Fuel Behaviour in Loss-of-coolant Accident (LOCA) Conditions," OECD Publications, Paris, France, 2009.

[4] S. Miwa, Y. Liu, T. Hibiki, M. Ishii, Y. Kondoh, N. Ukai and K. Tanimoto, "Experimental study of counter-current gas-droplet flow limitation in a 30 cm pipe," *Chemical Engineering Science,* vol. 92, pp. 167-179, 2013.

[5] J. A. Findlay, "BWR Refill-Reflood Program Task 4.4 - CCFL/Refill System Effects Test (30-degree Sector) Evaluation of ECCS Mixing Phenomena," U.S. Nuclear Regulatory Commission, Washington, DC, 1983.

[6] A. Yamanouchi, "Effect of Core Spray Cooling in Transient State after Loss of Coolant Accident," *Journal of Nuclear Science and Technology,* vol. 5:11, pp. 547-558 , 1968.

[7] J. D. Duncan and J. E. Leonard, "Emergency Cooling in BWR's Under Simulated Loss-of-Coolant Conditions (BWR-FLECHT Final Report)," General Electric, 1971.

[8] *Title 10 Code of Federal Regulations Part 50 Appendix K.*

[9] I. Choutapalli and K. Vierow, "Wall pressure measurements of flooding in vertical countercurrent annular air–water flow," *Nuclear Engineering and Design,* vol. 240:10, pp. 3221-3230, October 2010.

[10] U.S. Nuclear Regulatory Commission, "Compendium of ECCS Research for Realistic LOCA Analysis Final Report," U.S. Nuclear Regulatory Commission, Washington, DC, 1988.

[11] T. Eckert, "BWR Refill-Reflood Program- Core Spray Distribution Experimental Task Plan," Electric Power Research Institute, San Jose, CA, 1981.

[12] N. O. Jansson and H. Zhao, "Verification of GOBLIN-BE Versus SVEA Spray Cooling Test," in *Transactions of the ASME, Heat Transfer Divison*, 1992.

[13] S. Racca and T. Kozlowski, "Trace Code Validation for BWR Spray Cooling Injection and CCFL Condition Based on GOTA Facility Experiments," *Science and Technology of Nuclear Installations,* vol. 2012, pp. 1-17, 2012.

[14] W. Jaeger and V. H. S. Espinoza, "Uncertainty and Sensitivity Study in the Frame of TRACE Validation for Reflood Experiment," *Nuclear Technology,* vol. 184, pp. 333-350, 2013.

[15] M. O. Bäckwall and H. Wijkström, "SVEA Spray Cooling Test: Comparison with Current Swedish Licensing Methods," ASEA-ATOM, 1987.

[16] R. Eklund and M.-O. Bäckwall, "SVEA Spray Cooling Tests. Result from Test 012 (Matrix 11)," Asea-Atom, 1986.

[17] R. Eklund and M.-O. Bäckwall, "SVEA Spray Cooling Tests. Result from Test 015 (Matrix 14)," Asea-Atom, 1986.

[18] U.S. Nuclear Regulatory Commission, *TRACE V5.0 Theory Manual,* 2012, p. 372.

[19] Y. H. Cheng, J. Rwang, C. Shih and H. T. Lin, "A study of steam-water countercurrent flow model in TRACE code," in *Proceedings of the 17th International Conference on Nuclear Engineering*, Brussels, Belgium, 2009.

[20] B. Adams, M. Ebeida, M. Eldred, J. Jakeman, L. Swiler, J. A. Stephens, D. Vigil, T. Wildey, W. Bohnhoff, K. Dalbey, J. Eddy, K. Hu, L. Bauman and P. Hough, "Dakota, A Multilevel Parallel Object-Oriented Framework for Design Optimization, Parameter Estimation, Uncertainty Quantification, and Sensitivity Analysis: Version 6.2 User's Manual," Sandia National Laboratories, Albuquerque, New Mexico, 2015.

[21] T. Wickett, F. D'Auria and H. Glaese, "Report of the uncertainty method study for advanced best estimate thermalhydraulic codes applications," Vol. I OECD/CSNI NEA/CSNI Report R (97) 35, Paris, France, 1998.

[22] F. D'Auria, A. Bousbia-Salah, A. Petruzzi and A. Del Nevo, "State of the Art in Using Best Estimate Calculation Tools in Nuclear Technology," *Nuclear Engineering and Technology,* vol. 38, no. 1, pp. 11-32, 2006.

[23] B. Neykov, F. Aydogan, L. Hochreiter, K. Ivanov, H. Utsono, F. Kasahara, E. Sartori and M. Martin, "NUPEC BWR Full-Size Fine-Mesh Bundle Test ~BFBT Benchmark!. Volume II: Uncertainty and Sensitivity Analyses of Void Distribution and Critical Power— Specification," Nuclear Energy Agency, 2007.

[24] G. B. Wallis, One-dimensional two-phase flow, New York: McGraw-Hill, 1969.

[25] A. Kovtonyuk, A. Petruzzi and F. D'Auria, "Post-BEMUSE Reflood Model Input Uncertainty Methods (PREMIUM) Benchmark Phase II: Identification of Influential Parameters," Nuclear Energy Agency, 2014.

[26] M. S. El-Genk, B. Su and Z. Guo, "Experimental Studies of Forced, Combined and Natural Convection of Water in Vertical Nine-Rod Bundles with a Square Lattice," *International Journal of Heat Mass Transfer,* vol. 36, pp. 2359-2374, 1993.

[27] U.S. NRC, "TRACE V5.0 Assessment Manual: Main Report," U.S. Nuclear Regulatory Commission, Washington, D.C..

[28] D. C. Groeneveld, L. K. H. Leung, P. L. Kirillov, V. P. Bobkov, I. Smogalev, V. N. Vinogradov, X. C. Huang and E. Royer, "The 1995 look-up table for critical heat flux in tubes," *Nuclear Engineering and Design,* vol. 163, pp. 1-23, 1996.

[29] M. Ishii and I. Kataoka, "Interfacial transfer in Annular Dispersed Flow," *Advances in Two-Phase Flow and Heat Transfer ,* vol. 63, pp. 93-118, 1983.

[30] D. Zigrang and N. Sylvester, "Explicit Approximations to the Solution of Colebrook's Friction Factor Equation," *AIChE Journal,* vol. 28, no. 3, p. 514, 1982.

[31] S. S. Wilks, "Determination of Sample Sizes for Setting Tolerance Limits," *Annals of Mathematical Statistics,* vol. 12, no. 91, 1941.

[32] J. S. Chiou and L. E. Hochreiter, "COBRA/TF Analysis of SVEA Spray Cooling Experiments," in *Heat Transfer Phenomena in Radiation, Combustion and Fires*, Philadelphia, PA, 1989.

[33] U.S. Nuclear Regulatory Commission, "TRACE v5.840 User's Manual Volume 1: Input Specification," 2014.

[34] N. E. Todreas and M. S. Kazimi, Thermal Hydraulic Fundamentals, Hemisphere Publishing Corporation, 1990.

[35] R. Petterson, "GÖTA Data Analysdis: SKI Project B 39/77 Comparisons between test data and calcuations," ASEA-ATOM, 1979.

[36] R. W. Griebe and J. W. McConnell, "Boiling Water Reactor - Full Length Emergency Core Cooling Heat Transfer (BWR-FLECHT) Tests Project Final Report on Atmospheric Pressure Stainless Steel Experiments," Aerojet Nuclear Company, Idaho Falls, Idaho, 1973.

[37] *Title 10 Code of Federal Regulations Part 50.46.*

[38] T. R. Smith, J. P. Schlegel, T. Hibiki and M. Ishii, "Mechanistic modeling of interfacial area transport in large diameter pipes," *International Journal of Multiphase Flow,* vol. 47, pp. 1-16, 2012.